

A PROGRAM FOR CALCULATING THE REFLECTIVITY OF BEACH PROFILES

BY

JAMES T. KIRBY

March 1987

Sponsor:

Office of Naval Research



COASTAL & OCEANOGRAPHIC ENGINEERING DEPARTMENT

UNIVERSITY OF FLORIDA

Gainesville, Florida 32611

REPORT DOCUMENTATION PAGE

1. Report No.	2.	3. Recipient's Accession No.	
4. Title and Subtitle A Program for Calculating the Reflectivity of Beach Profiles		5. Report Date	
7. Author(s) James T. Kirby		6. 8. Performing Organization Report No. UFL/COEL-87/004	
9. Performing Organization Name and Address Coastal and Oceanographic Engineering Department University of Florida 336 Weil Hall Gainesville, FL 32611		10. Project/Task/Work Unit No.	
12. Sponsoring Organization Name and Address Office of Naval Research		11. Contract or Grant No. N00014-86-K-0790	
15. Supplementary Notes		13. Type of Report Miscellaneous	
14.		16. Abstract	
<p>This report documents a program for computing the reflection of linear water waves propagating over a one-dimensional, arbitrary topography. The restrictions of linear theory are assumed to apply. Dissipative effects and wave breaking are also neglected. The program is used in several examples pertaining to the design and construction of artificial, reflective bar fields on mildly-sloping beaches.</p>			
17. Originator's Key Words Nearshore bars Wave reflection		18. Availability Statement	
19. U. S. Security Classif. of the Report Unclassified	20. U. S. Security Classif. of This Page Unclassified	21. No. of Pages 47 pp	22. Price

A PROGRAM FOR CALCULATING THE REFLECTIVITY OF BEACH PROFILES

BY

JAMES T. KIRBY

March 1987

Sponsor:

Office of Naval Research

A Program for Calculating the Reflectivity of Beach Profiles¹

James T. Kirby
Coastal and Oceanographic Engineering Department
University of Florida
Gainesville, FL 32611

UFL/COEL-87/004
March, 1987

¹This work was supported by the Office of Naval Research, Contract number N00014-86-K-0790

Abstract

This report documents a program for computing the reflection of linear water waves propagating over a one-dimensional, arbitrary topography. The restrictions of linear theory are assumed to apply. Dissipative effects and wave breaking are also neglected. The program is used in several examples pertaining to the design and construction of artificial, reflective bar fields on mildly-sloping beaches.

Contents

1	Introduction	1
2	Theory	2
3	Numerical Approximations	6
4	Model Tests and Examples	10
4.1	Reflection from sinusoidal bars	10
4.2	Reflection from arrays of semicircular bars	15
4.3	Artificial bar field on a sloping beach	24
4.4	Discussion of computational limitations	30
5	Program Listing	33
6	References	43

List of Figures

1	Definition of depth components	2
2	Sinusoidal bottom, $m = 4, D/h = 0.32$. Data from Davies and Heathershaw (1984)	11
3	Sinusoidal bars as in Figure 2. 45° angle of incidence	12
4	Reflection and transmission for geometry for Figure 2; varying wave period and angle of incidence.	14
5	Reflection from row of semicircular bars. $m = 4$, regular spacing	16
6	Bottom variation spectra for regularly spaced semicircular bars.	17
7	Effect of irregular bar spacing on reflection by semicircular bars.	20
8	Bar geometries corresponding to Figure 7.	21
9	Spectra for irregular-spaced bar configurations.	22
10	Reflection from regular array of semicircular bars, $2m$ spacing	23
11	Configuration of artificial bars on a sloping beach	24
12	Reflection and transmission for regularly spaced bars on a sloping beach. . .	26
13	Reflection and transmission for irregular bar spacing on a sloping beach. . .	27
14	Reflection from a sloping beach. $80m$ bar spacing.	28
15	Reflection from a sloping beach. $20m$ bar spacing.	29
16	Reflection and transmission for regular and irregular bar spacing on a sloping beach, LLW+1.61m.	32

1 Introduction

The amount of wave energy arriving at a shoreline after propagation over offshore bathymetry is affected by a number of mechanisms leading to loss of energy flux relative to values measured at an offshore station. The mechanisms of bottom damping have long been under investigation, and may significantly reduce the amount of wave energy arriving at the surf zone. Recently, the possible influence of the reflectivity of the beach profile has come under closer scrutiny. In particular, several recent studies (Davies and Heathershaw (1984); Mei (1985)) have shown that undular bottom features mimicking shore-parallel bars can lead to strong reflection of incident surface waves. The existence of this mechanism provides a means for approaching the design of artificial, bar-like structures intended to significantly reduce wave energy arriving at the shore.

This report documents a program which may be used to calculate the reflection of linear water waves by a specified offshore topography. By building up results for individual frequency and directional components, the program can compute the transfer function for the reflection of a spectrum with directional and frequency spread. The theoretical and numerical approaches are summarized in sections 2 and 3. Section 4 then provides several examples of the use of the program. A program listing and documentation are provided in section 5.

2 Theory

The theory which serves as the basis for development of the computer program described here is taken directly from the work of Kirby(1986). Kirby developed an extension to the mild-slope equation of Berkhoff (1972) which allows the equation to be applied to bottoms having a slowly-varying mean depth on which is superimposed a rapidly-varying but small-amplitude depth change. The smallness of the rapid variation allows the bottom boundary conditions to be expanded about the slowly - varying mean depth. Following the notation in Kirby, we take the total depth $h'(x, y)$ to be expressed by

$$h'(x, y) = h(x, y) - \delta(x, y) \quad (1)$$

where h satisfies a mild-slope condition and δ satisfies a small-amplitude condition. The split of the total local depth into components is illustrated in Figure 1. The resulting

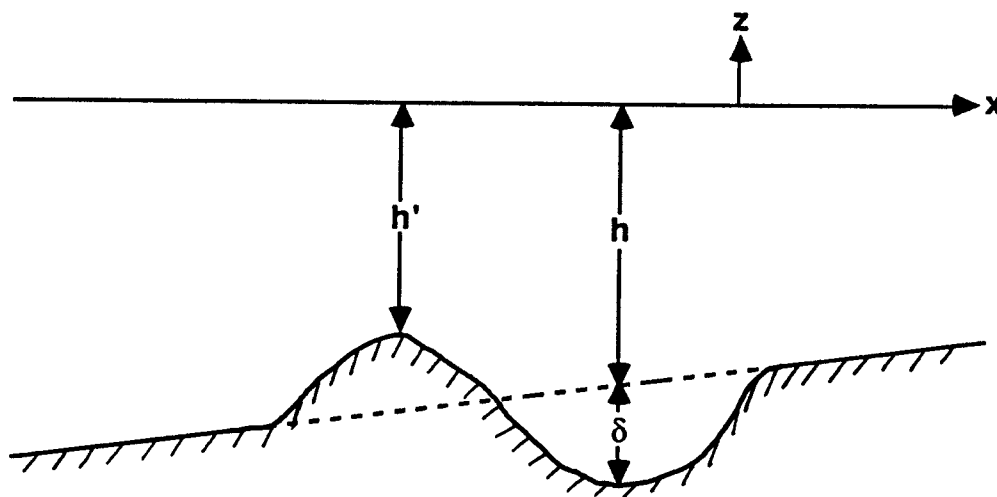


Figure 1: Definition of depth components

extension to the mild-slope equation is then given by

$$\tilde{\phi}_{tt} - \nabla \cdot (CC_g \nabla \tilde{\phi}) + (\omega^2 - k^2 CC_g) \tilde{\phi} + \frac{g}{\cosh^2 kh} \nabla \cdot (\delta \nabla \tilde{\phi}) = 0. \quad (2)$$

Here, $\tilde{\phi}$ represents the velocity potential in the plane of the free surface, and is related to a three-dimensional velocity potential ϕ according to

$$\phi(x, y, z, t) = \frac{\cosh k(h+z)}{\cosh kh} \tilde{\phi}(x, y, t) \quad (3)$$

Equation (2) is valid for a single frequency component of a linear wave train, with frequency ω and wavenumber k related by

$$\omega^2 = gk \tanh kh \quad (4)$$

The remaining coefficients are determined from (4) and are given by

$$C = \frac{\omega}{k} \quad (5)$$

$$C_g = \frac{\partial \omega}{\partial k} = \frac{\omega}{2k} \left(1 + \frac{2kh}{\sinh 2kh} \right) \quad (6)$$

In the absence of currents, $\tilde{\phi}$ is also simply related to the surface displacement η through a simple constant of proportionality, and hence η may be substituted in (2) in place of $\tilde{\phi}$. We make this substitution. We then consider the case of purely harmonic motion and introduce a spatial surface displacement $\tilde{\eta}$ according to

$$\eta(x, y, t) = \tilde{\eta}(x, y) e^{-i\omega t} \quad (7)$$

This substitution reduces (2) to the form

$$\nabla \cdot (CC_g \nabla \tilde{\eta}) + k^2 CC_g \tilde{\eta} - \frac{g}{\cosh^2 kh} \nabla \cdot (\delta \nabla \tilde{\eta}) = 0. \quad (8)$$

We now restrict the model to the case of one dimensional topography;

$$h'(x) = h(x) - \delta(x) \quad (9)$$

The full elliptic problem (8) is further reduced to

$$CC_g (\nabla^2 \tilde{\eta} + k^2 \tilde{\eta}) + (CC_g)_x \tilde{\eta}_x - \frac{g\delta}{\cosh^2 kh} \nabla^2 \tilde{\eta} - \frac{g}{\cosh^2 kh} \delta_x \tilde{\eta}_x = 0. \quad (10)$$

We now treat the two-dimensional surface $\tilde{\eta}$ as a spectrum of directional wave components which individually refract over the slowly-varying topography $h(x)$ according to Snell's law. For a given component which is incident at angle θ_0 in deep water, we have the relation

$$k \sin \theta = k_0 \sin \theta_0 \quad (11)$$

where

$$k_0 = \frac{\omega^2}{g} \quad (12)$$

We denote local wavenumber vector components according to

$$l = k \cos \theta \quad (13)$$

$$m = k \sin \theta = k_0 \sin \theta_0 \quad (14)$$

where m is evidently a constant for all x . We also obtain the relation

$$k^2 = l^2 + m^2 \quad (15)$$

Noting that $m \leq k_0$ from (14), if decaying modes are to be neglected, we may write $\tilde{\eta}$ formally as

$$\tilde{\eta} = \int_{-k_0}^{k_0} \hat{\eta}(x, m) e^{im y} dm \quad (16)$$

Substituting (16) in (10) then yields a second-order ODE for the $\hat{\eta}(m)$;

$$(CC_g \hat{\eta}_x)_x - \frac{g}{\cosh^2 kh} (\delta \hat{\eta}_x)_x + \left[l^2 CC_g + \frac{gm^2 \delta}{\cosh^2 kh} \right] \hat{\eta} = 0. \quad (17)$$

Equation (17) gives a well-posed problem for the reflection of each individual direction component after the specification of boundary conditions. Formally, the problem may be posed in the interval $-\infty < x \leq 0$, where $x = 0$ represents the shoreline and the wave is incident from the deep ocean at $-\infty$. This problem is intractable. In order to simplify the problem, we suppose that the incident wave condition is known at some finite distance x_1 from the shoreline. Further, we neglect the region of the surfzone and take a second station x_2 to represent a position between the region of topography of interest and the breaker

zone. We then assume that wave energy transmitted past station x_2 is lost to breaking. This assumption implies the neglect of direct reflection at the shoreline, which may become an important effect on steep beaches or on shores fronted by seawalls or other reflective structures. We thus consider only the problem of (17) posed in a finite domain $x_1 \leq x \leq x_2$ together with boundary conditions given at x_1 and x_2 ; the resulting reflection coefficients will not contain the effect of shoreline reflection.

Boundary conditions are developed in the form of radiation conditions. At x_2 , we assume that the wave is propagating out of the finite domain towards the shoreline, in the $+x$ direction. We thus take

$$\hat{\eta}_x = il(x)\hat{\eta}; \quad x = x_2 \quad (18)$$

At the offshore station x_2 , the wavefield is composed of the incident component $\hat{\eta}_i$, which is assumed to be known, and a reflected component $\hat{\eta}_r$, which must satisfy a radiation condition for propagation out of the domain:

$$\hat{\eta}_{rx} = -il(x)\hat{\eta}_r; \quad x = x_1 \quad (19)$$

Noting that

$$\hat{\eta}_r = \hat{\eta} - \hat{\eta}_i \quad (20)$$

we substitute (20) in (19) and obtain

$$\hat{\eta}_x = il(2\hat{\eta}_i - \hat{\eta}); \quad x = x_1 \quad (21)$$

(17) together with (18) and (21) fully specifies the problem to be solved.

3 Numerical Approximations

We now develop a finite-difference scheme for solving the problem posed by (17), (18) and (21). We drop the $\hat{}$ superscript notation for $\eta(x, m)$ and further define the notations

$$p = CC_g \quad (22)$$

$$\gamma = \frac{g}{\cosh^2 kh} \quad (23)$$

We then discretize the domain $x_1 \leq x \leq x_2$ into n points according to

$$x^i = x_1 + (i - 1)\Delta x; \quad 1 \leq i \leq n \quad (24)$$

where

$$\Delta x = \frac{x_2 - x_1}{n - 1} \quad (25)$$

All other coefficients and the dependent variable η are defined in discrete form at the grid points x^i . We then develop a centered finite-difference scheme for (17) which is given by

$$\begin{aligned} & \frac{(p^{i+1} + p^i)(\eta^{i+1} - \eta^i) - (p^i + p^{i-1})(\eta^i - \eta^{i-1})}{2\Delta x^2} \\ & - \gamma^i \frac{(\delta^{i+1} + \delta^i)(\eta^{i+1} - \eta^i) - (\delta^i + \delta^{i-1})(\eta^i - \eta^{i-1})}{2\Delta x^2} \\ & + [(l^i)^2 p^i + m^2 \gamma^i \delta^i] \eta^i = 0. \end{aligned} \quad (26)$$

(26) may be written in the simple form

$$A^i \eta^{i-1} + B^i \eta^i + C^i \eta^{i+1} = 0; \quad i = 2, \dots, n - 1 \quad (27)$$

where

$$A^i = p^i + p^{i-1} - \gamma^i (\delta^i + \delta^{i-1}) \quad (28)$$

$$\begin{aligned} B^i &= -(p^{i+1} + 2p^i + p^{i-1}) + \gamma^i (\delta^{i+1} + 2\delta^i + \delta^{i-1}) \\ & \quad + 2\Delta x^2 [(l^i)^2 p^i + m^2 \gamma^i \delta^i] \end{aligned} \quad (29)$$

$$C^i = p^{i+1} + p^i - \gamma^i (\delta^{i+1} + \delta^i) \quad (30)$$

We note that, in the special case where waves are started in shallow water and then propagated to deeper water, l given by

$$l = \sqrt{k^2 - m^2} \quad (31)$$

may become imaginary, which represents a turning point in the mathematical problem and a caustic in the physical refraction problem. The problem is generally formulated to handle this case by allowing the appropriate variables to have complex form.

We now turn to the boundary conditions. In order to simplify the application of the boundary condition and the determination of reflection and transmission coefficients, we assume that the input topography $h(x^i)$ has been modified to give a flat bottom at the edges of the domain;

$$\begin{aligned} h^1 &= h^2 \\ h^{n-1} &= h^n \end{aligned} \quad (32)$$

In keeping with this restriction, we require $\delta(x)$ to have compact support in the domain $x_1 \leq x \leq x_2$, so that the waves at the radiating boundary are not interacting with rapid bed undulations. We thus require

$$\delta^1 = \delta^2 = \delta^{n-1} = \delta^n = 0. \quad (33)$$

We then finite difference the transmitting boundary condition (18) in centered form according to

$$\frac{\eta^n - \eta^{n-1}}{\Delta x} = \frac{i l^n}{2} \eta^n + \frac{i l^n}{2} \eta^{n-1} \quad (34)$$

where $l^{n-1} = l^n$ due to (32) above. Let

$$\alpha^n = \frac{i \Delta x}{2} l^n. \quad (35)$$

(34) may then be written as

$$\eta^n(1 - \alpha^n) = \eta^{n-1}(1 + \alpha^n) \quad (36)$$

or, in the notation of (27),

$$\begin{aligned} B^n &= 1 - \alpha^n \\ A^n &= -(1 + \alpha^n) \end{aligned} \quad (37)$$

The reflective boundary condition is handled in a similar way. Defining

$$\alpha^1 = \frac{i\Delta x}{2} l^1, \quad (38)$$

we obtain

$$(1 + \alpha^1)\eta^2 - (1 - \alpha^1)\eta^1 = 2a(m)\alpha^1 [e^{2\alpha^1} + 1] \quad (39)$$

where we have assumed that the incident wave is specified by

$$\eta_i(x) = a(m)e^{i l^1(x-x_1)} \quad (40)$$

We then have

$$B^1 = -(1 - \alpha^1) \quad (41)$$

$$C^1 = 1 + \alpha^1 \quad (42)$$

$$D^1 = 2a(m)\alpha^1 [e^{2\alpha^1} + 1] \quad (43)$$

The entire problem may then be written in the form of a linear matrix equation

$$\mathbf{A}\eta = \mathbf{D} \quad (44)$$

where \mathbf{D} is a column vector with $D^2 - D^n = 0$, η is a column vector with elements $\eta^1 - \eta^n$, and \mathbf{A} is a tridiagonal matrix with diagonal vectors A^i , B^i and C^i . The solution is obtained using the double sweep algorithm as given by Carnahan, Luther and Wilkes (1969).

After determining the solution for η , the reflection and transmission coefficients must be determined. At x_1 , we obtain two estimates of the reflection coefficient R as follows. Using (40), we may write η_r at x_1 as

$$\begin{aligned} \eta_r^1 &= \eta^1 - a(m) \\ \eta_r^2 &= \eta^2 - a(m)e^{2\alpha^1} \end{aligned} \quad (45)$$

We then take

$$\begin{aligned} R_1 &= \frac{|\eta_r^1|}{a(m)} \\ R_2 &= \frac{|\eta_r^2|}{a(m)} \end{aligned} \quad (46)$$

R is then estimated as the simple average of R_1 and R_2 . Similarly, at x_2 we obtain estimates of transmission coefficient T according to

$$\begin{aligned} T_1 &= \frac{|\eta^{n-1}|}{a(m)} \\ T_2 &= \frac{|\eta^n|}{a(m)} \end{aligned} \quad (47)$$

and then average T_1 and T_2 to obtain T . A test of the accuracy of the solution is obtained by checking the conservation of energy requirement

$$R^2 + T^2 \left(\frac{C_g^n l^n k^1}{C_g^1 l^1 k^n} \right) = 1. \quad (48)$$

The results for an entire frequency and directional spectrum may be built up by repeated application of the numerical scheme developed here. A program corresponding to the present numerical algorithm is documented in section 5 below.

4 Model Tests and Examples

In this section, we provide an adequate set of tests of the present program in comparison to previous results, and then test several cases of interest in the problem of constructing an artificial nearshore bar field. The first set of tests pertain to the familiar problem of wave reflection by a sinusoidal bar field, as studied recently by Davies and Heathershaw (1984), Mei (1985) and Kirby (1986).

4.1 Reflection from sinusoidal bars

Davies and Heathershaw have obtained a detailed set of measurements of wave reflection from a sinusoidal topography given by

$$\delta(x) = D \sin(\lambda x); \quad 0 \leq x \leq L \quad (49)$$

where $\lambda = 2\pi/l_b$, l_b is the bar length, and $L = ml_b$. The bar field thus contains m complete sinusoidal bars. Tests were run with $l_b = 1m$, $D = 0.05m$ and $m = 2, 4$ or 10 . Mean depth $h(x)$ was uniform so that the bars were superimposed on a domain with otherwise constant depth. Wave period T and water depth h were varied during the tests to obtain the range of parameters desired. Figure 2 shows computed reflection (solid line) and transmission (dashed line) coefficients for a case with $m = 4$ and $h = D/0.32 = 0.15625m$ for normally-incident waves. Also included in the figure is the laboratory data of Davies and Heathershaw. Reflection associated with the presence of a beach downwave of the ripple patch is estimated to be on the order of 0.2, accounting for much of the discrepancy between theory and data away from resonance. Agreement between the approximate theory of Davies and Heathershaw and the present numerical results is quite close, deviating the most at the resonant peak. (This fact is probably due to Davies and Heathershaw's treatment of the resonance in their theory; see the discussion in the introduction of Kirby (1986).) Agreement between present numerical results and other sets of laboratory data presented by Davies and Heathershaw was also good and additional results are thus not shown.

Existing theories for resonant (Mei, 1985) and non-resonant (Miles, 1981) reflection of

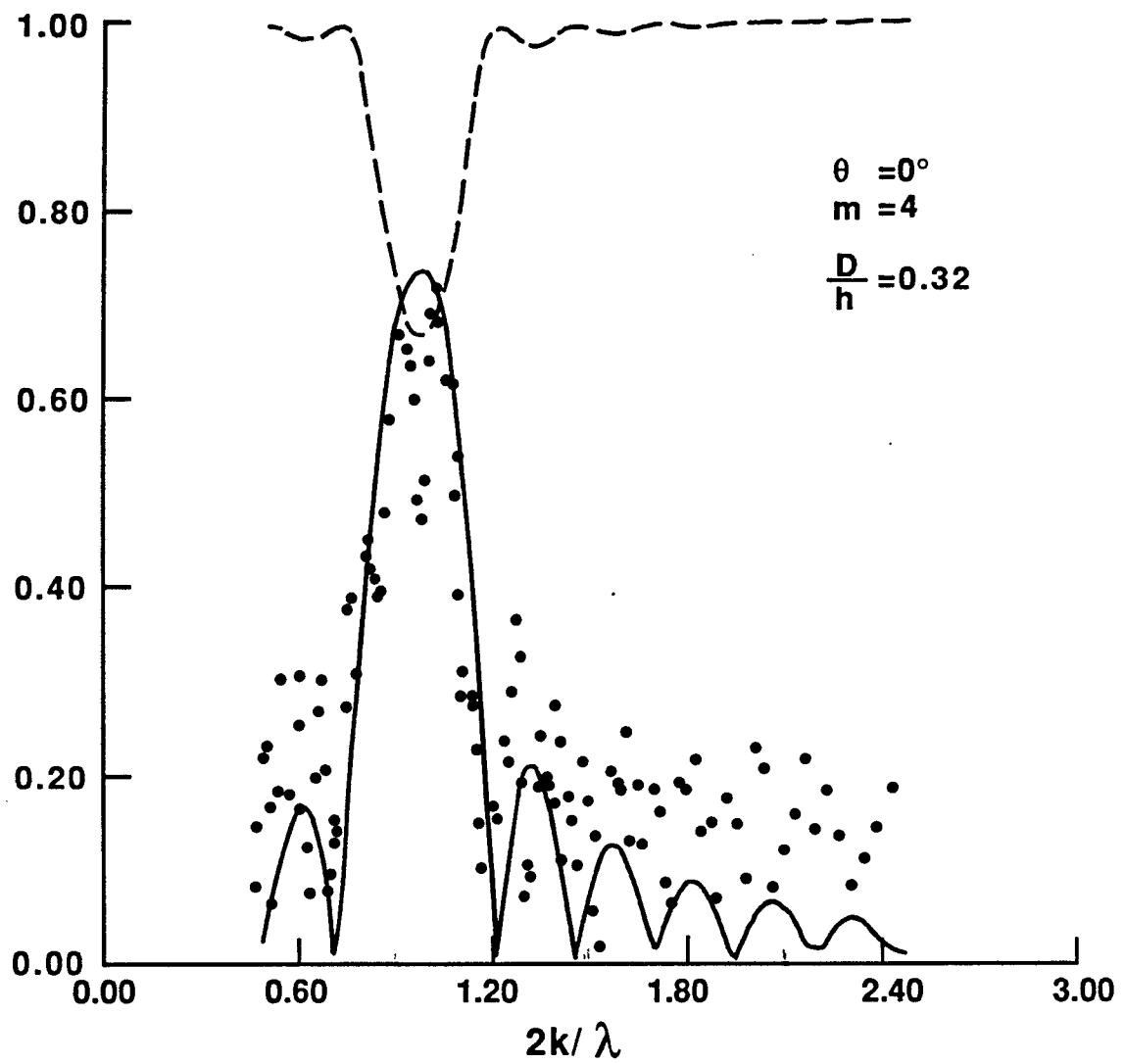


Figure 2: Sinusoidal bottom, $m = 4$, $D/h = 0.32$. Data from Davies and Heathershaw (1984)

obliquely incident waves over topography $\delta(x)$ all predict a zero in the incident-reflected wave coupling at an angle of incidence of 45° . This result indicates that the bar field is transparent to waves at this angle, at least at leading order. Figure 3 shows an example of results for a 45° angle of incidence and the geometry of Figure 2. The reflection coefficient is non-zero but is not sufficiently large to reduce transmission by a significant amount.

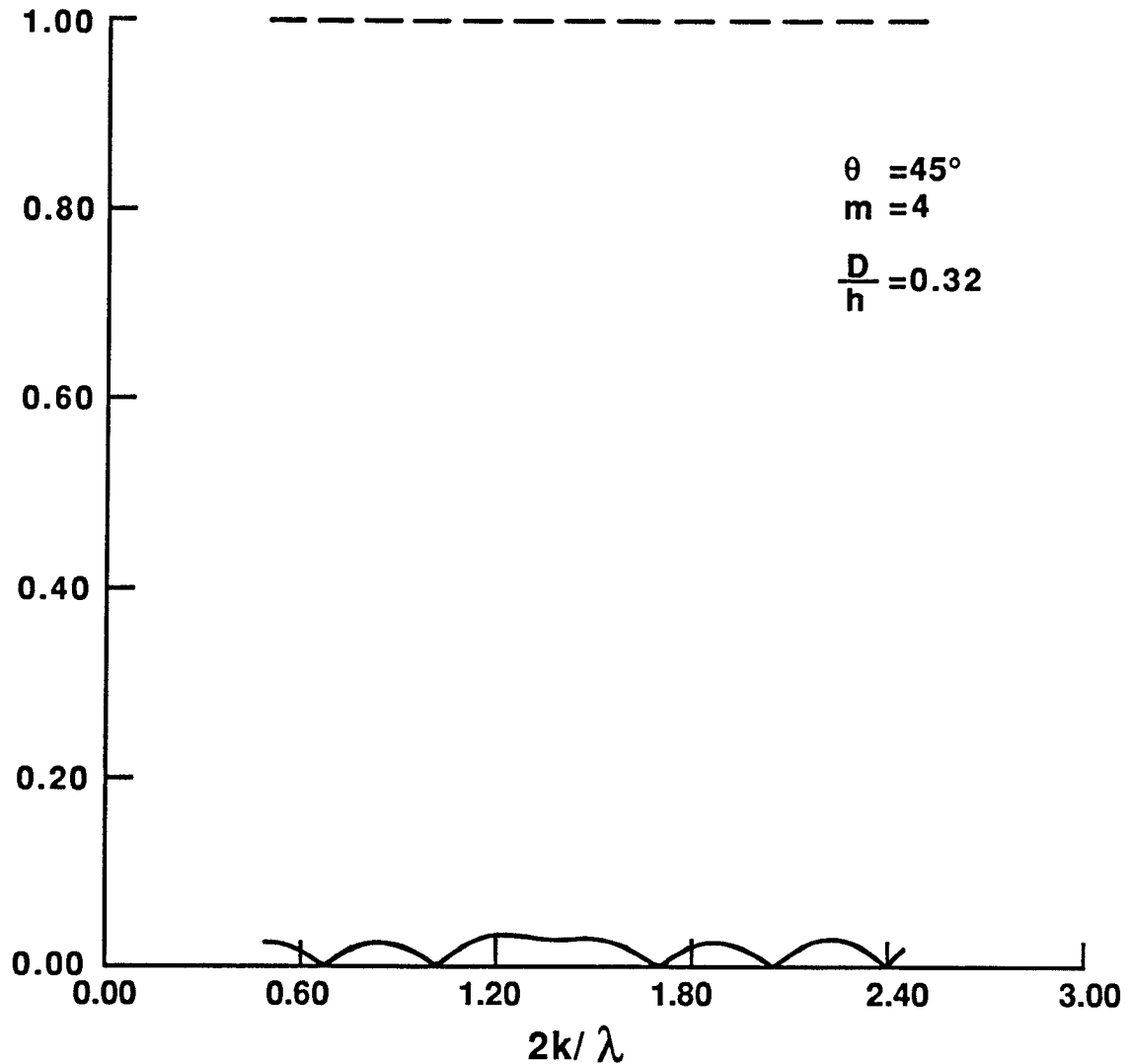


Figure 3: Sinusoidal bars as in Figure 2. 45° angle of incidence

Figure 4 shows a contour plot of reflection and transmission coefficients for a range of wave periods and angles of incidence for the geometry of Figure 2. The region of effec-

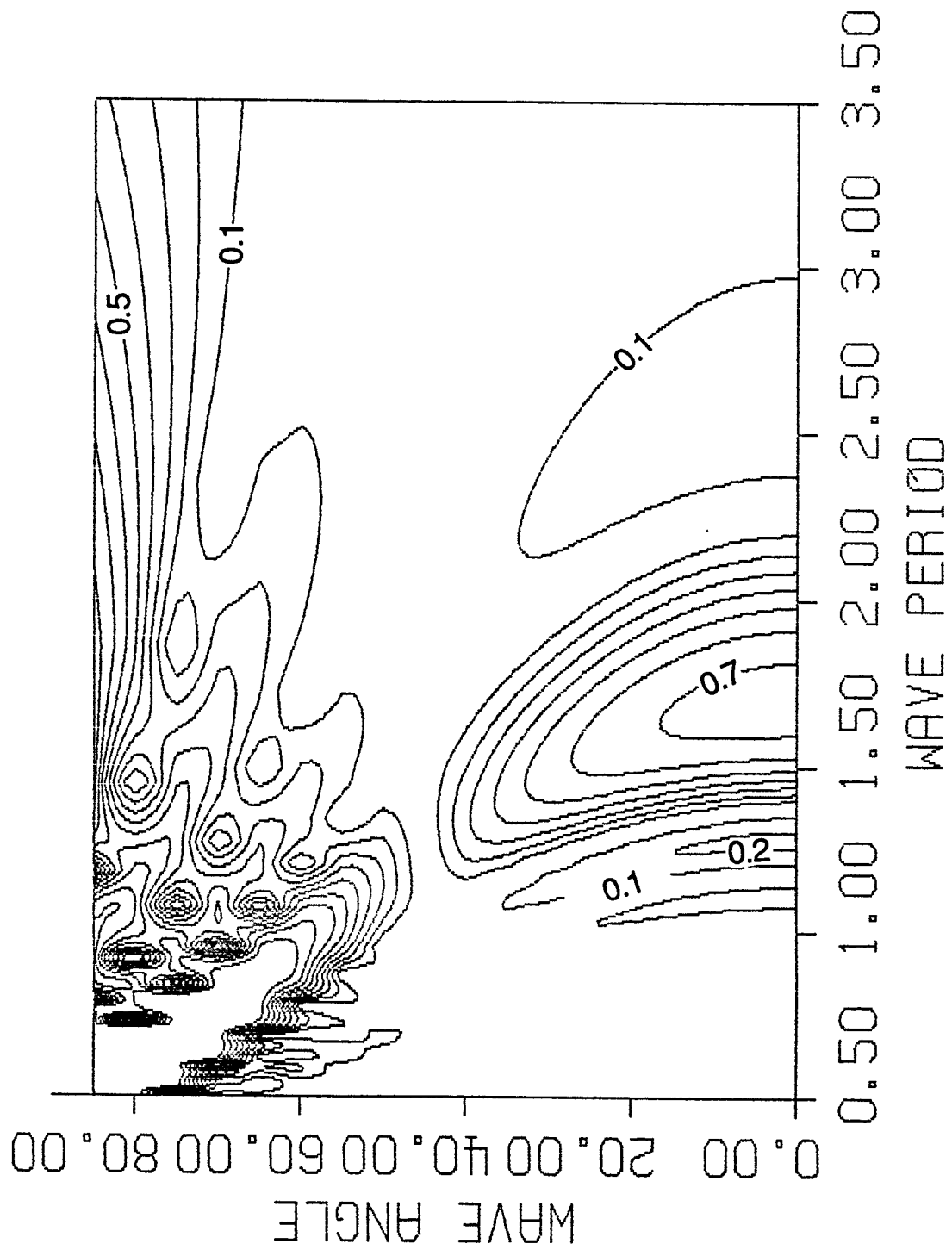
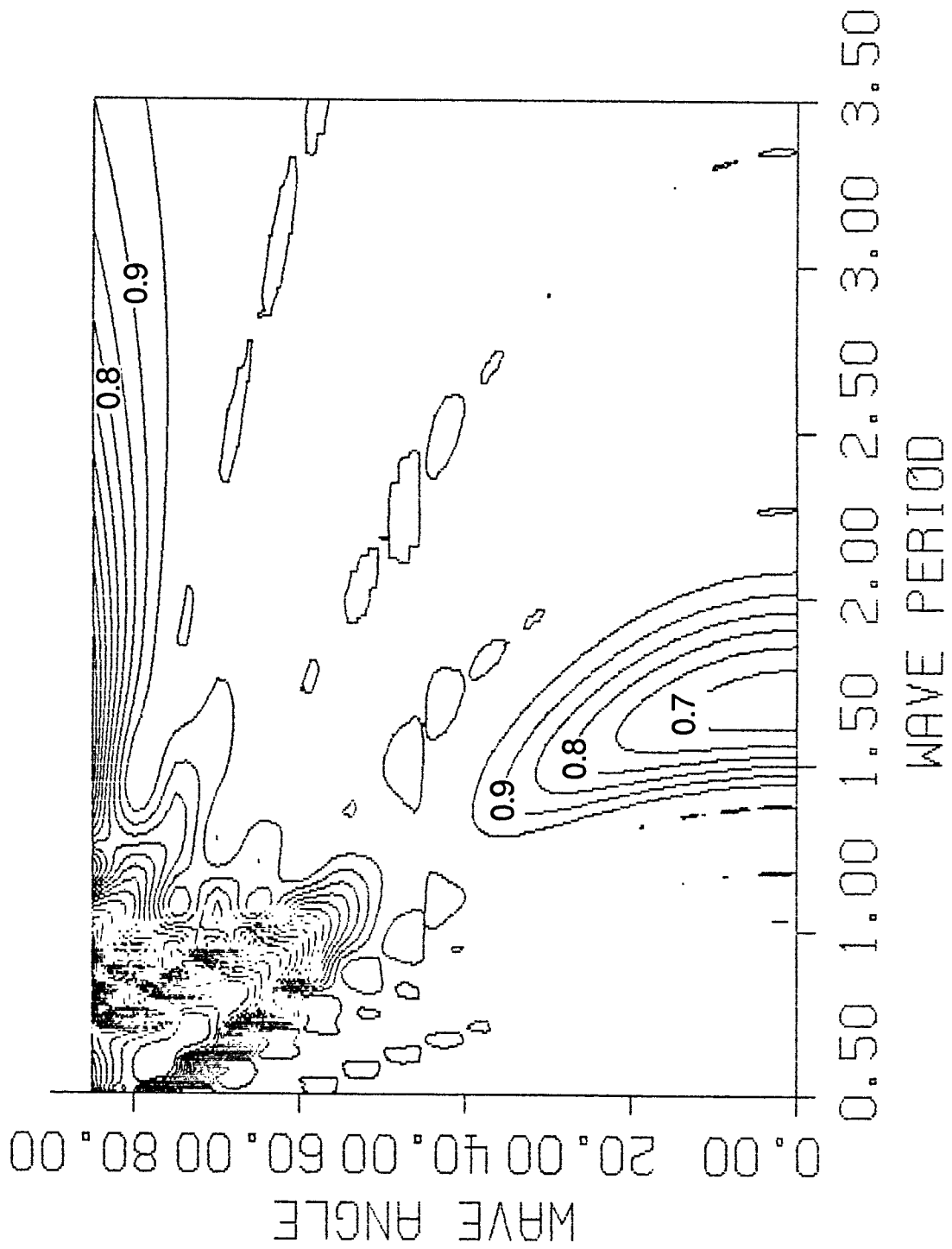


Figure 4. a) Reflection coefficient



b) Transmission coefficient

Figure 4: Reflection and transmission for geometry for Figure 2; varying wave period and angle of incidence.

tive reduction of transmission is localized to the patch $0 \leq \theta \leq 45^\circ$ around the resonant wavenumber, except for regions of strong reflection at large angles of incidence.

4.2 Reflection from arrays of semicircular bars

Construction of an artificial bar field which mimics the reflective behavior of a patch of sinusoidal bars will likely involve the placement of several discrete structures whose longitudinal axes run parallel to shore and whose on-offshore spacing is controlled. In this section, we look at several examples of bar fields consisting of rows of semicircular structures placed on an otherwise flat bottom. The case of bars placed on a sloping bottom is left to the next section.

For a given run, all bars are assumed to have the same radius r ; $\delta(x)$ for x in the interval of a bar location is then given by

$$\delta(x) = [r^2 - |x - x_b|^2]^{1/2} \quad (50)$$

where x_b is the bar center location. We first test a regularly spaced field of 4 bars with a spacing of 1 m and a water depth of $h = 0.15625m$. We take $r = 0.05m$. This case thus mimics the sinusoidal geometry for Figure 2, with bar crests having the same spacing and the same vertical projection above the horizontal bottom. Results are shown in Figure 5, where we retain the same definition for λ as in the previous section.

The results for the field of semicircular bars exhibit several interesting features. The reflection peak at $2k/\lambda = 1$ is still present and represents the Bragg-interaction of the wave train with the fundamental spacing of the bar field. A second, stronger peak is present at $2k/\lambda = 2$ and represents the Bragg interaction of the wave train with the first superharmonic spacing of the bar field. These results need to be interpreted in light of the Fourier transform of the constructed depth profile. The basic periodic interval for the transform analysis is indicated in Figure 6a, and the FFT amplitude spectrum corresponding to the interval is shown in Figure 6b. The spectrum of the bottom drops off quite slowly above the fundamental component, which would be the only component present in an ideal

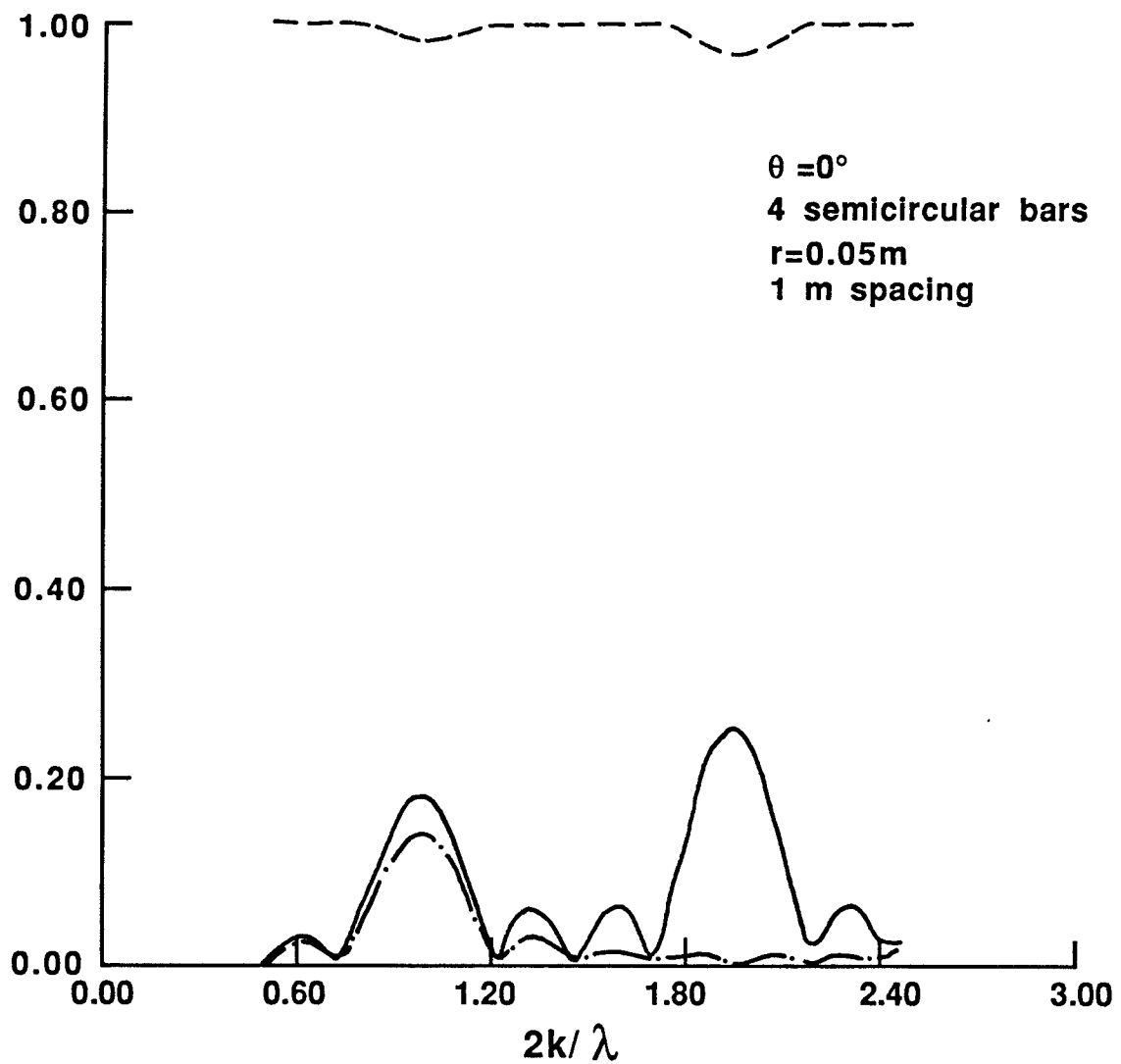
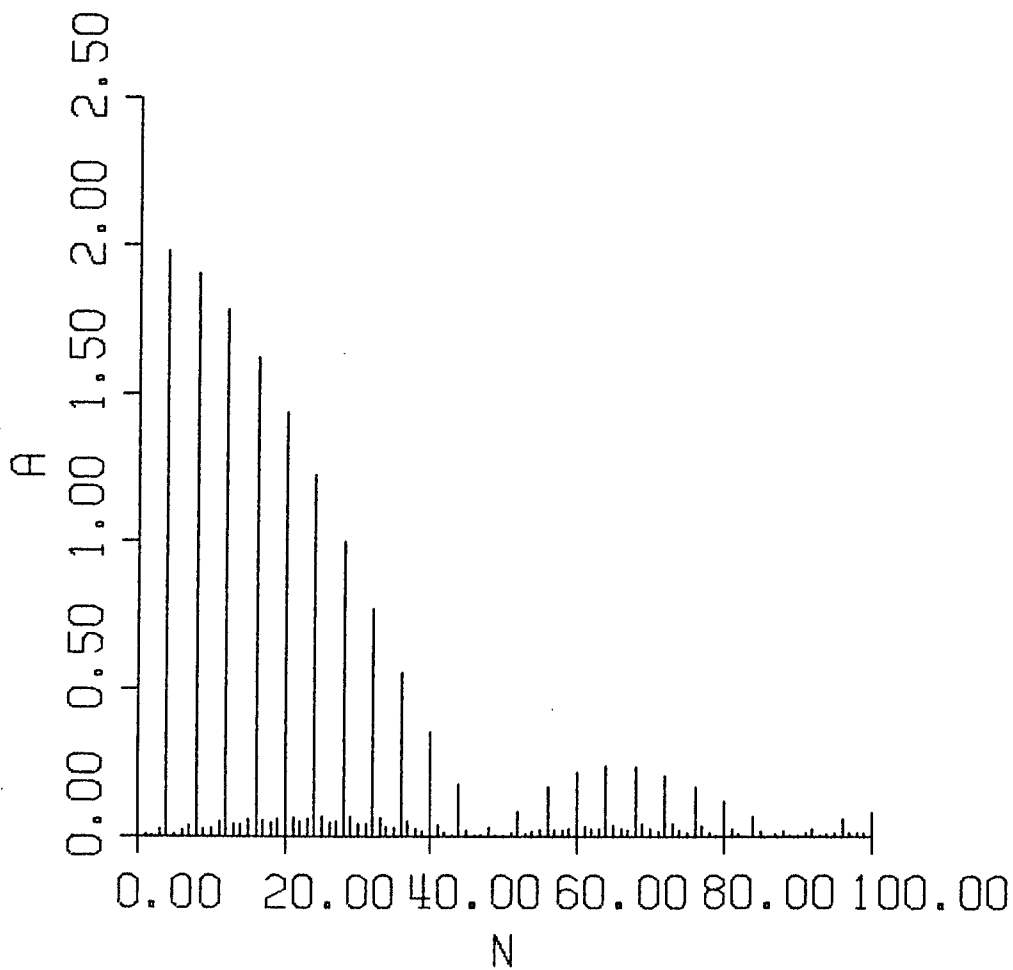


Figure 5: Reflection from row of semicircular bars. $m = 4$, regular spacing



a) periodic bottom interval



b) amplitude spectra of bottom variation

Figure 6: Bottom variation spectra for regularly spaced semicircular bars.

sinusoidal bottom. This indicates that the reflection response should be spread over a broad band of wavenumbers, with intensified response occurring near the spectral peaks of the bottom variation. (Compare to the case of a single discrete rectangular bump, for which the spectrum is nearly white and the reflection coefficient varies nearly sinusoidally with wavelength). The drawback to this particular type of broadening of the reflection response is that much of the bottom variance is dedicated to reflecting wave components which are outside the range of wave periods where reflection is to be concentrated. It would be more efficient from a design point of view to devise a bottom configuration which concentrated the bottom variance in spectral components corresponding to the band of surface waves of interest. The practicality of constructing such arrangements, which would tend back towards the sinusoidal configuration, is doubtful.

The amplitude variance associated with the first spectral component of the regularly-spaced bar configuration corresponds to a sinusoidal bar with amplitude $0.008m$. Reflection from such a bar field was computed and is shown in Figure 5 as the dash-dot line. It is apparent that most of the reflection near peaks of the response is associated with Bragg-reflection from the individual bottom spectral components, but that non-resonant interaction with other components of the bar field can overlap the region of resonant response, causing a shift in the apparent peak amplitude. Kirby (1986) has shown that the reflection in the vicinity of a resonant peak for one particular bottom component is almost equal to the simple sum of the reflection contributions from all spectral components. (See, in particular, Figures 5 and 6 in Kirby (1986)).

The results above raise the question of whether bar fields consisting of relatively abrupt, isolated structures should be constructed with a dominant spacing equal to the dominant surface wavelength (or some other spacing), rather than to half the dominant wavelength as would be the case for a simple sinusoidal bottom. This hypothesis will be tested further below.

Another feature needing investigation is the effect of spacing the bars irregularly in

order to introduce an increased variety of spectral components in the bottom topography, thus broadening the reflection response. Figures 7a-d show 4 examples obtained by altering the spacings of the 4 bars corresponding to the Figure 5 example in such a way that the total bar field width of $3m$ is maintained. The result for uniform spacing is included in each figure as the dashed line. The bar field geometries corresponding to the 4 cases are indicated in Figure 8.

Spectra of bottom variations for the 4 irregularly spaced bar configurations are shown in Figure 9. The effect of irregular spacing is to produce a more densely populated bottom spectrum, thus increasing the number of spectral components which individually take part in Bragg-interactions with a broad surface wave spectrum. It is not immediately apparent from the plotted spectra that an optimum choice of spacing distortion can be made, and thus this problem remains to be treated from an analytic point of view.

We now return to the question of constructing a bar field with a dominant spacing other than the $1/2$ -wavelength spacing indicated by the direct Bragg-resonance mechanism. We first test a spacing of one wavelength (relative to the Bragg condition in Figures 2 and 5), which, for the regularly spaced bars of Figure 5, corresponds to a $2m$ uniform spacing. The resulting reflection response is plotted in Figure 10. Comparing these results to Figure 5, we see that the main effect of lengthening the bar field by a factor of two is to sharpen the resonant tuning associated with harmonics of the bottom variation. The resonant peak at $2k/\lambda = 1$ (with $\lambda = 2\pi$ as in Figure 5) now corresponds to the first harmonic of the basic periodicity, the fundamental now being located at $2k/\lambda = 0.5$. No shift in maximum amplitude of the resonant peaks is achieved. The response may be characterized as being less effective than the original Figure 5 response if a narrow band around $2k/\lambda = 1$ is the principal concern, or more effective due to the extra peak at $2k/\lambda = 1.5$ if broad-spectrum response is the major consideration.

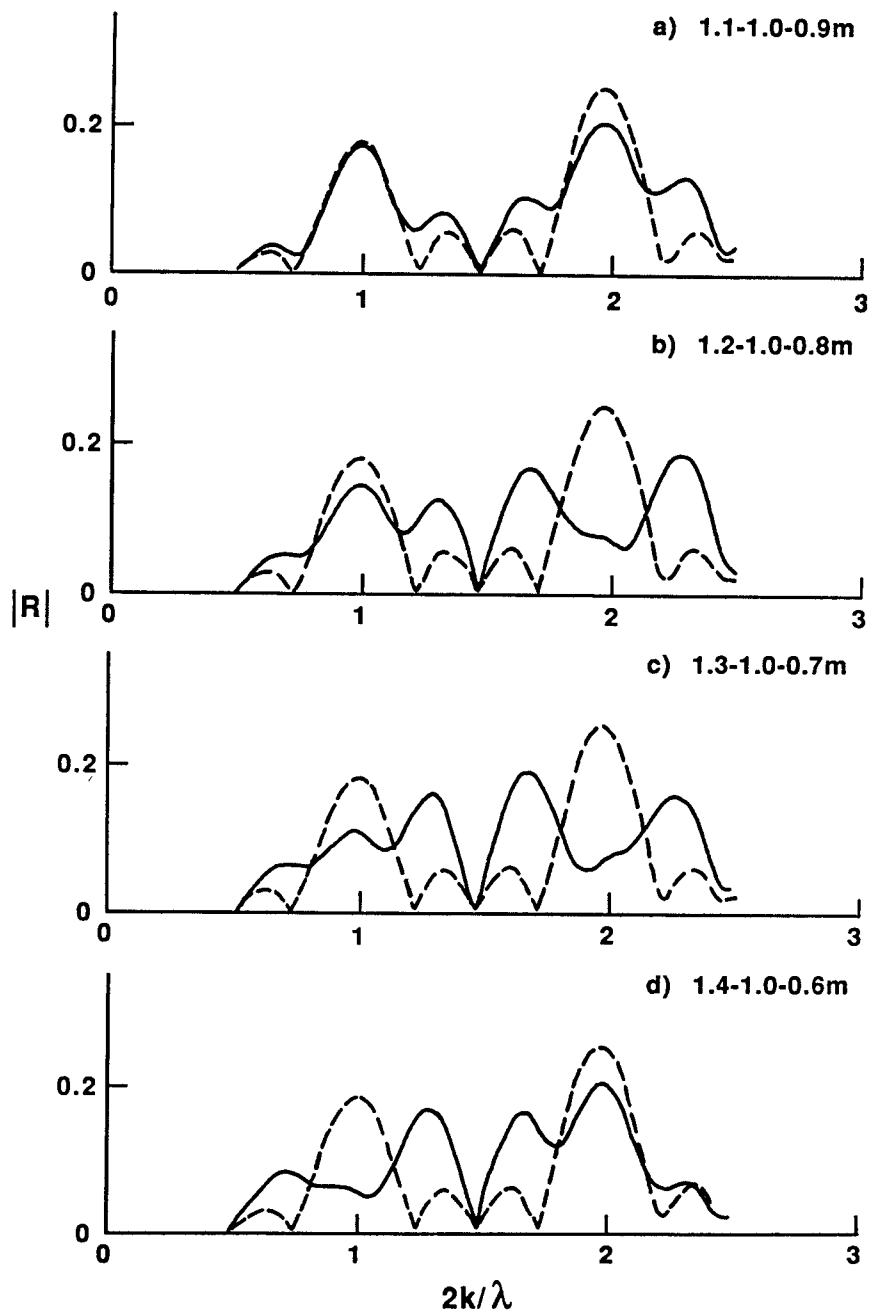


Figure 7: Effect of irregular bar spacing on reflection by semicircular bars.

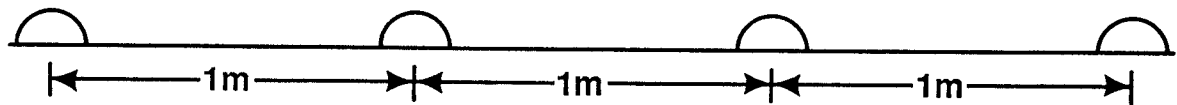


Figure 7a

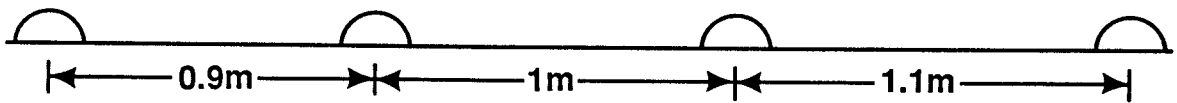


Figure 7b

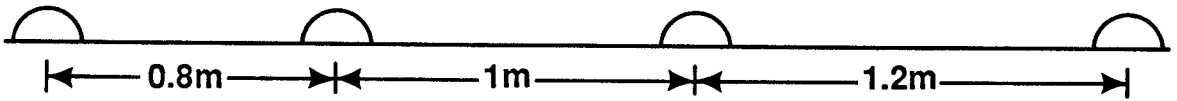


Figure 7c

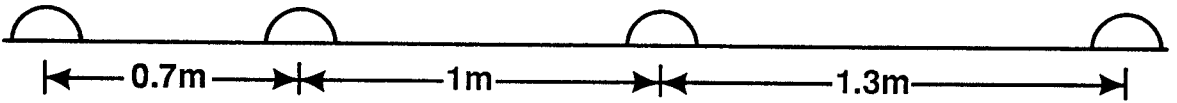


Figure 7d

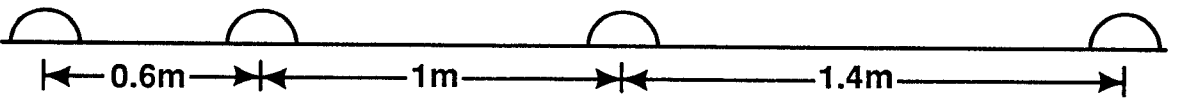


Figure 8: Bar geometries corresponding to Figure 7.

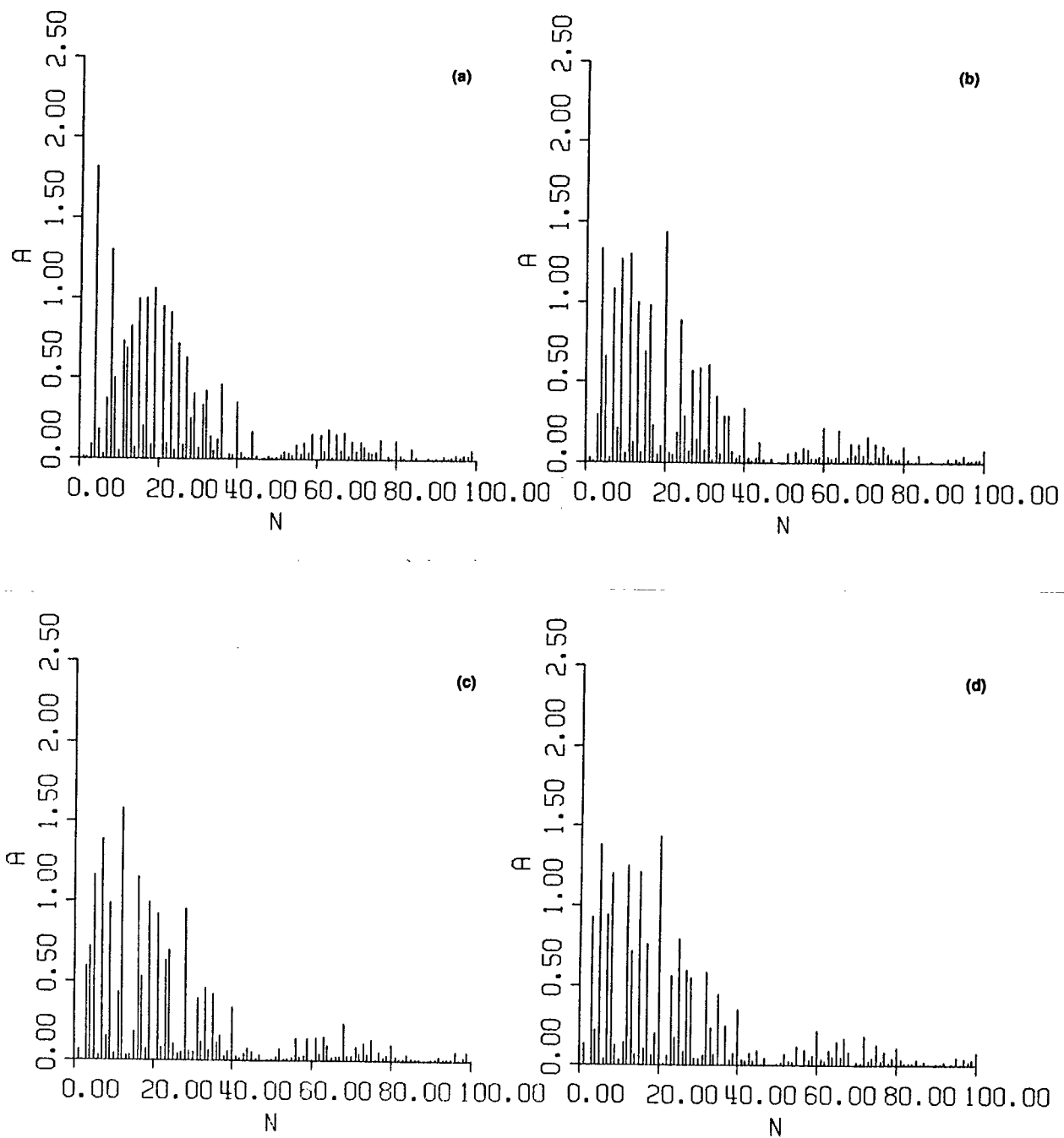


Figure 9: Spectra for irregular-spaced bar configurations.

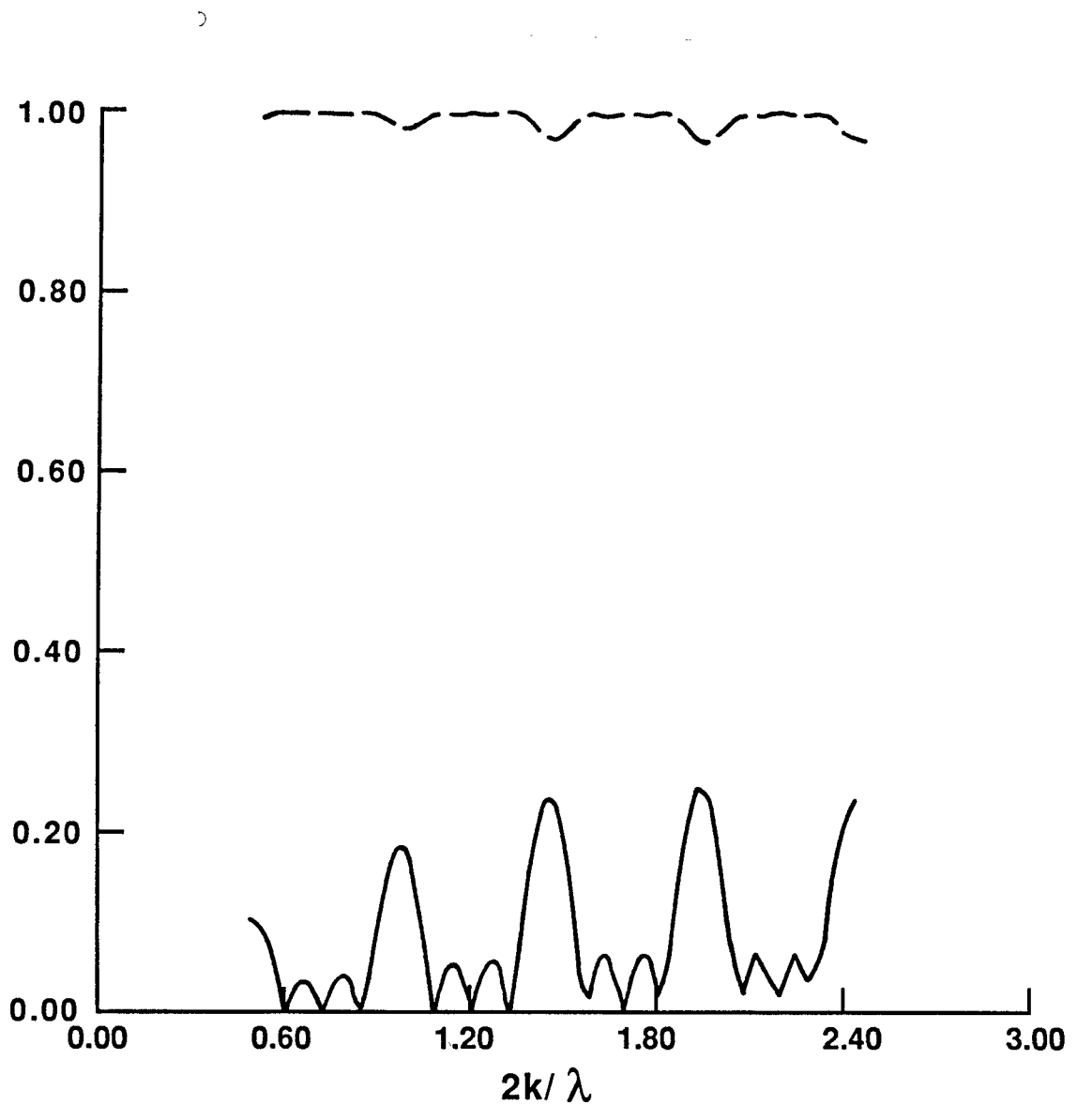


Figure 10: Reflection from regular array of semicircular bars, $2m$ spacing

4.3 Artificial bar field on a sloping beach

We now turn to a particular application of the present theory to a proposed bar field installation at Point Mugu beach. The profile geometry and bar field configuration are taken initially from the report by DeVries (1987). The only initial alteration to the proposed configuration is to impose a semicircular cross-section on the bars. The bar radius is taken to be $2m$ (~ 6 ft), corresponding to the 6 ft diameter proposed for circular obstacles. The initial configuration is indicated in Figure 11. The computational scheme was initialized

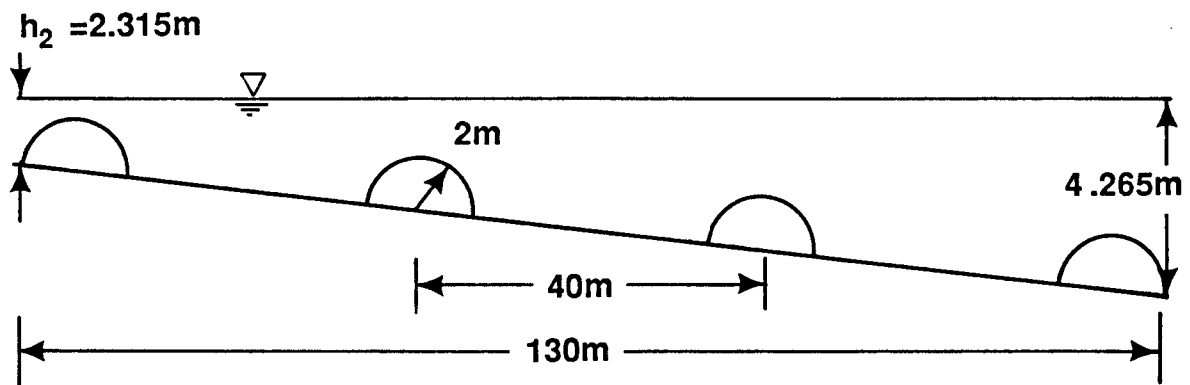


Figure 11: Configuration of artificial bars on a sloping beach

by taking a section of beach extending $5m$ shoreward of the shoreward bar center and $5m$ offshore of the offshore bar center. For an initial configuration of 4 bars at a nominal uniform spacing of $40m$ (~ 120 ft), the horizontal extent of the computational domain is $130m$. The LLWL depths at the onshore and offshore ends are $2.315 m$ and $4.265 m$, respectively, and the beach slope is 0.015.

An initial run was made with no bars in place to determine the reflectivity of the finite extent of the tested profile. Reflection was calculated for a range of wave periods from 5 to 20 seconds. The maximum reflection in this range was on the order of 0.02 and is not dynamically significant.

The first set of runs with bars was made with a water level of $LLW + 0.61m$, which corresponds to the level of the first profile break $100m$ seaward of the high-tide beach face. Figure 12 shows the reflection coefficient (solid line) and transmission coefficient referenced to the shoreward depth (short dashes) for the initial configuration of 4 bars at an equal spacing of $40m$, over a range of wave periods from $5sec$ to $20sec$. The main Bragg resonance peak is located near $T = 14sec$, and first and second superharmonic peaks are apparent at $T = 7.5sec$ and $T \approx 4.5sec$. The reflection response has a sharp drop off in the range $T = 10 - 11sec$, and the initial configuration is thus not well suited to the proposed storm condition with $T = 12sec$. (Response centered on the annual mean of $T = 14.69sec$ is significantly better).¹

In order to shift the Bragg-resonance peak more towards the $12sec$ storm period and broaden the overall response, a staggered array of 4 bars was tested next, with the shoreward and seaward bars at the same location and an internal spacing of $30m - 40m - 50m$. The response resulting from this spacing is shown in Figure 13. Staggering the spacing had the desired result of broadening the response characteristics with no concurrent reduction of the magnitude of reflection. This approach thus appears to be quite successful in the sloping beach application.

Two additional runs were performed in order to test the shifting of bar spacing as in the previous section. Figure 14 shows the reflection response for 4 bars at a uniform spacing of $80m$ (a rough one-wavelength/bar space in the $14sec$ band). The increased number of spectral peaks in the response is apparent as in the previous section, but the overall response drops off. This is likely to be due to the increase in depth over the seaward bars, which renders these bars less effective.

In Figure 15, the results for a regular spacing of $20m$ are shown (again using 4 bars). The main Bragg resonant peak is now shifted to $\sim 8sec$, and there is no spectral peak in the $10 - 15sec$ band. This case is not applicable to the West Coast site under investigation, but

¹(Wave data values from DeVries, 1987)

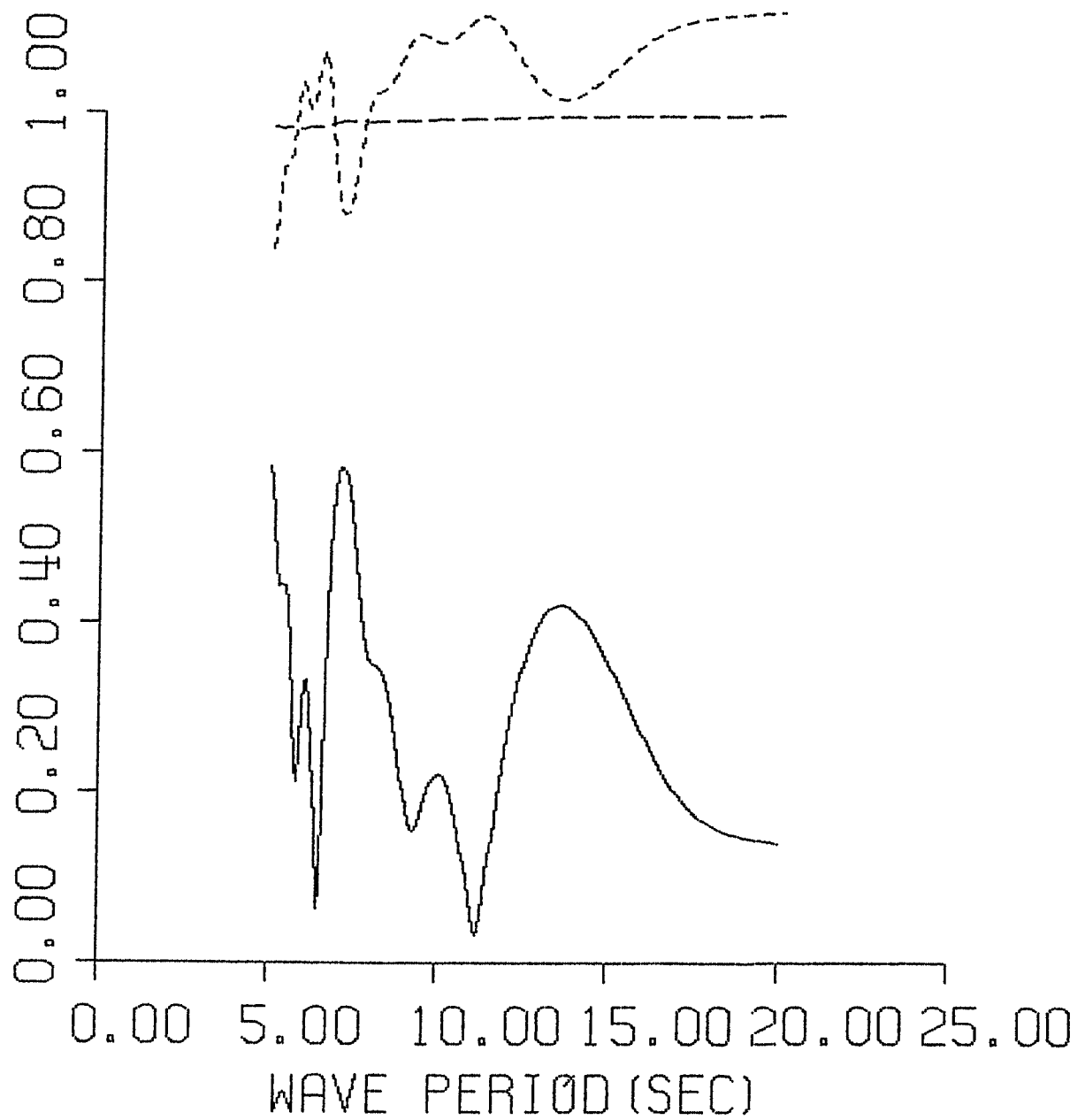


Figure 12: Reflection and transmission for regularly spaced bars on a sloping beach. Four bars, 40m spacing, LLW+0.61m

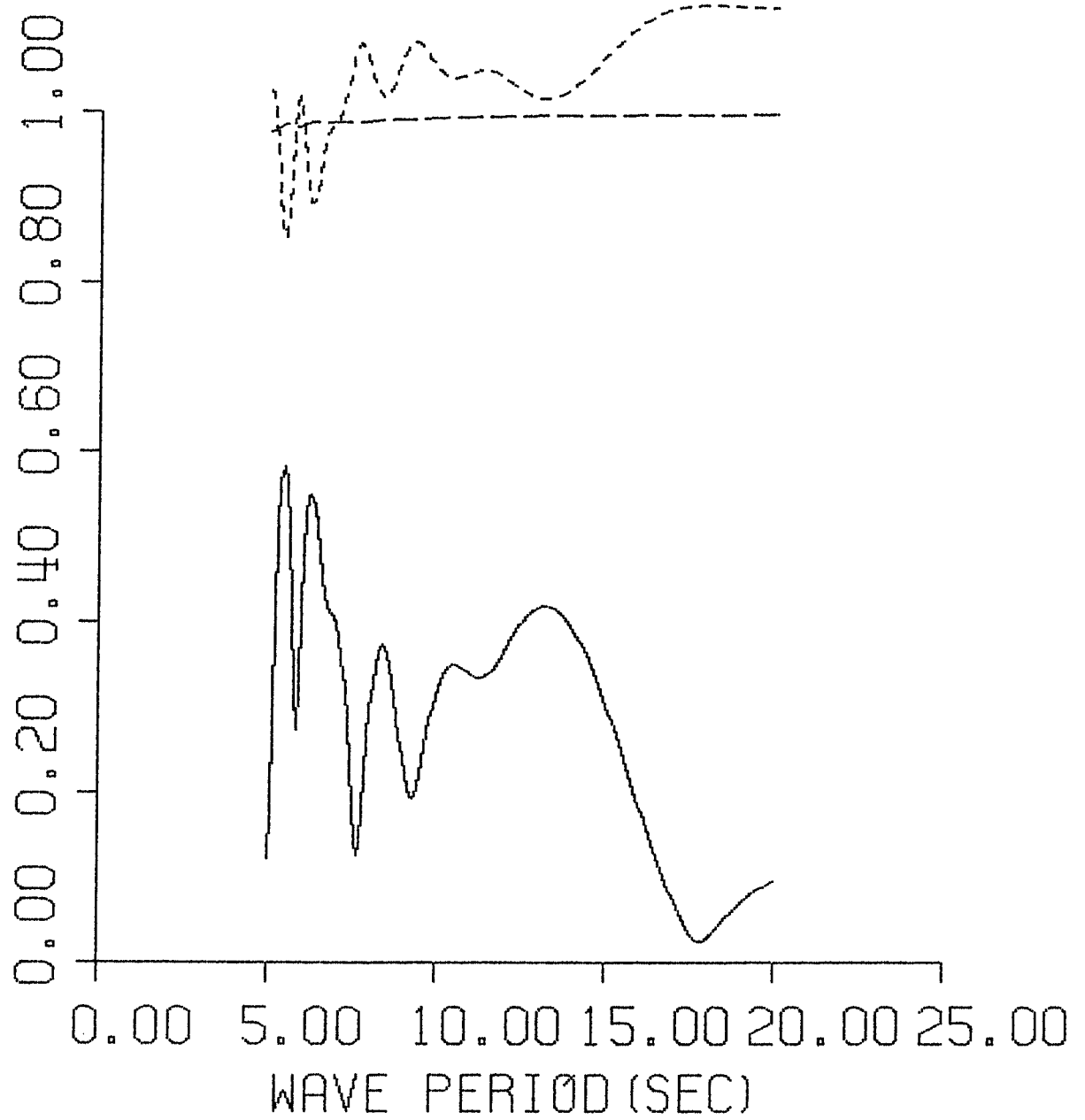


Figure 13: Reflection and transmission for irregular bar spacing on a sloping beach. Four bars, 30 - 40 - 50m spacing, LLW+0.61m.

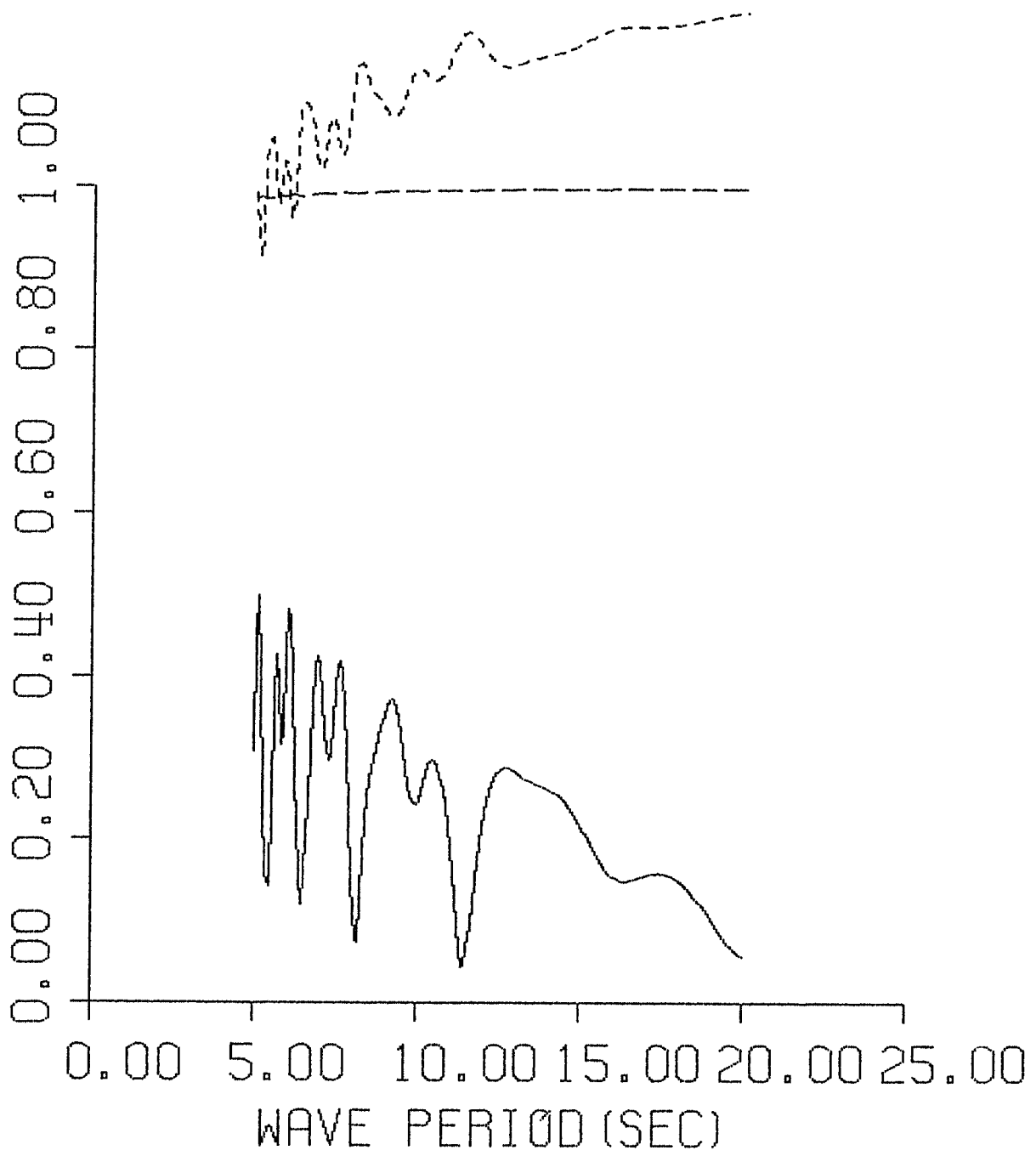


Figure 14: Reflection from a sloping beach. 80m bar spacing, LLW+0.61m.

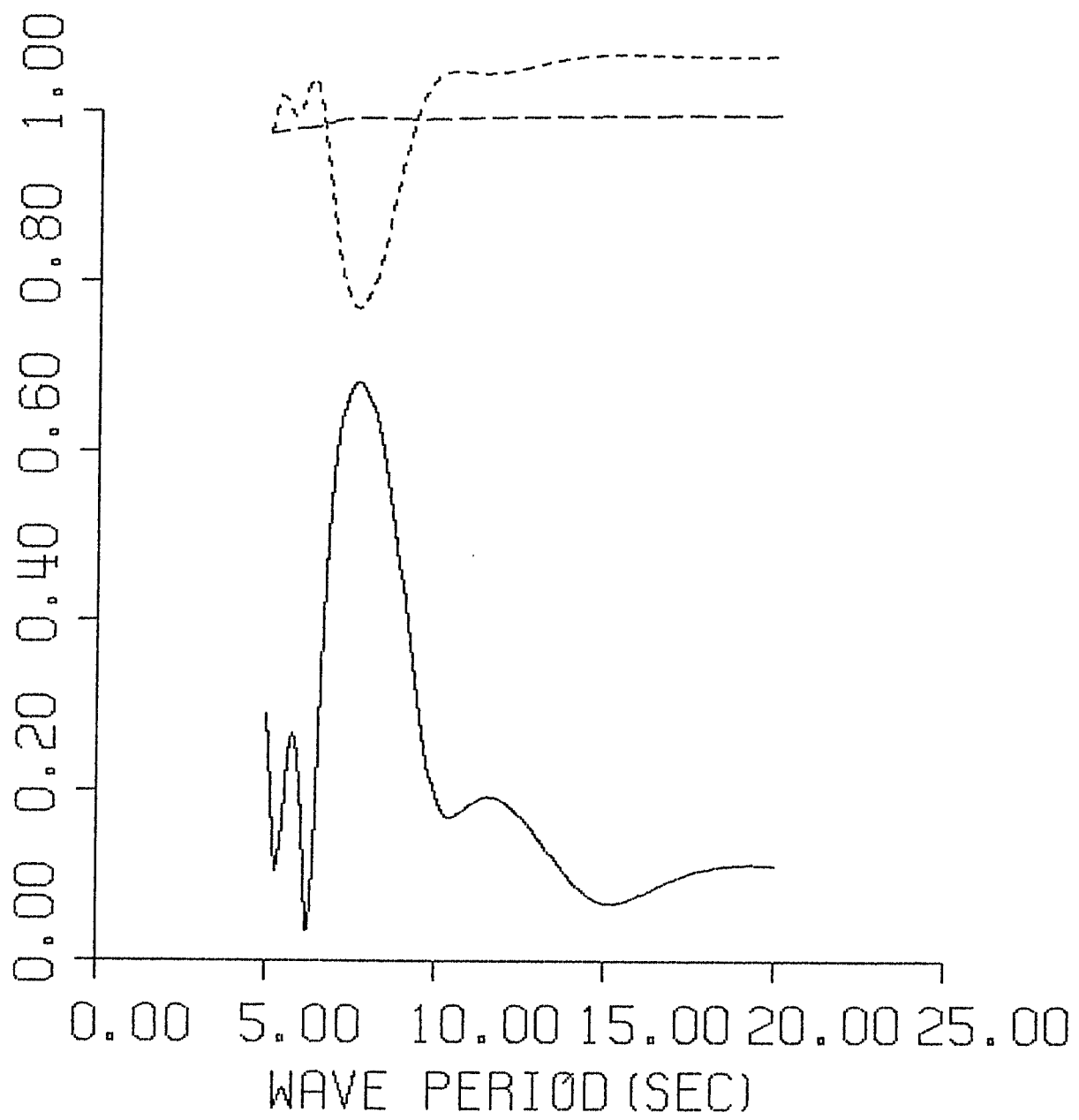


Figure 15: Reflection from a sloping beach. 20m bar spacing, LLW+0.61m.

gives an indication of what might be achieved on an East Coast site, where wave periods are shorter. In this case, quite a strong reflection can be achieved due to the fact that water depth over the bar field does not significantly change over the short spatial interval of the bar field.

Finally, the effect of tidal elevation on the response of a given configuration must be considered. Increasing tidal elevation causes greater submergence of the bar field and thus reduces the effectiveness of the reflection process. The change in depth/bar spacing also shifts the Bragg-resonant peak relative to a fixed range of wave periods. Figure 16 shows the response of the 4 bar array with 40 – 40 – 40m spacing and 30 – 40 – 50m spacing for a tidal elevation of LLW+1.61m. For the regular spacing, the peak is shifted down to $\sim 13sec$ from 14sec, and the overall magnitude of the reflection is dropped to ~ 0.2 from 0.4. For the irregular spacing, the response is still broad in comparison to the regularly-spaced bars, but the overall magnitude of the reflection is similar to the regular-spacing case, and the downshifts in wave period are also similar.

4.4 Discussion of computational limitations

For the bar fields considered here, two factors are likely to conflict with the goal of computational accuracy of the results. First, for tidal stages corresponding to LLW, submergence of the shoreward bar is slight and waves are likely to be breaking over the bar crest. This effect could possibly be incorporated in the model by adapting a breaking wave scheme from an empirical viewpoint, but strong nonlinearities would not be properly accounted for. Secondly, for the lower water levels tested, the bar height/water depth is as large as 0.7, and the perturbation scheme adopted here is invalidated. Previous results obtained by Dalrymple and Kirby (1986), using the boundary integral method for linear wave theory, have indicated that the present method starts to overpredict reflection as the limits of its validity are exceeded. It may be necessary to develop the boundary integral method for the cases studied here in order to obtain estimates of reflection for configurations having shallow submergence.

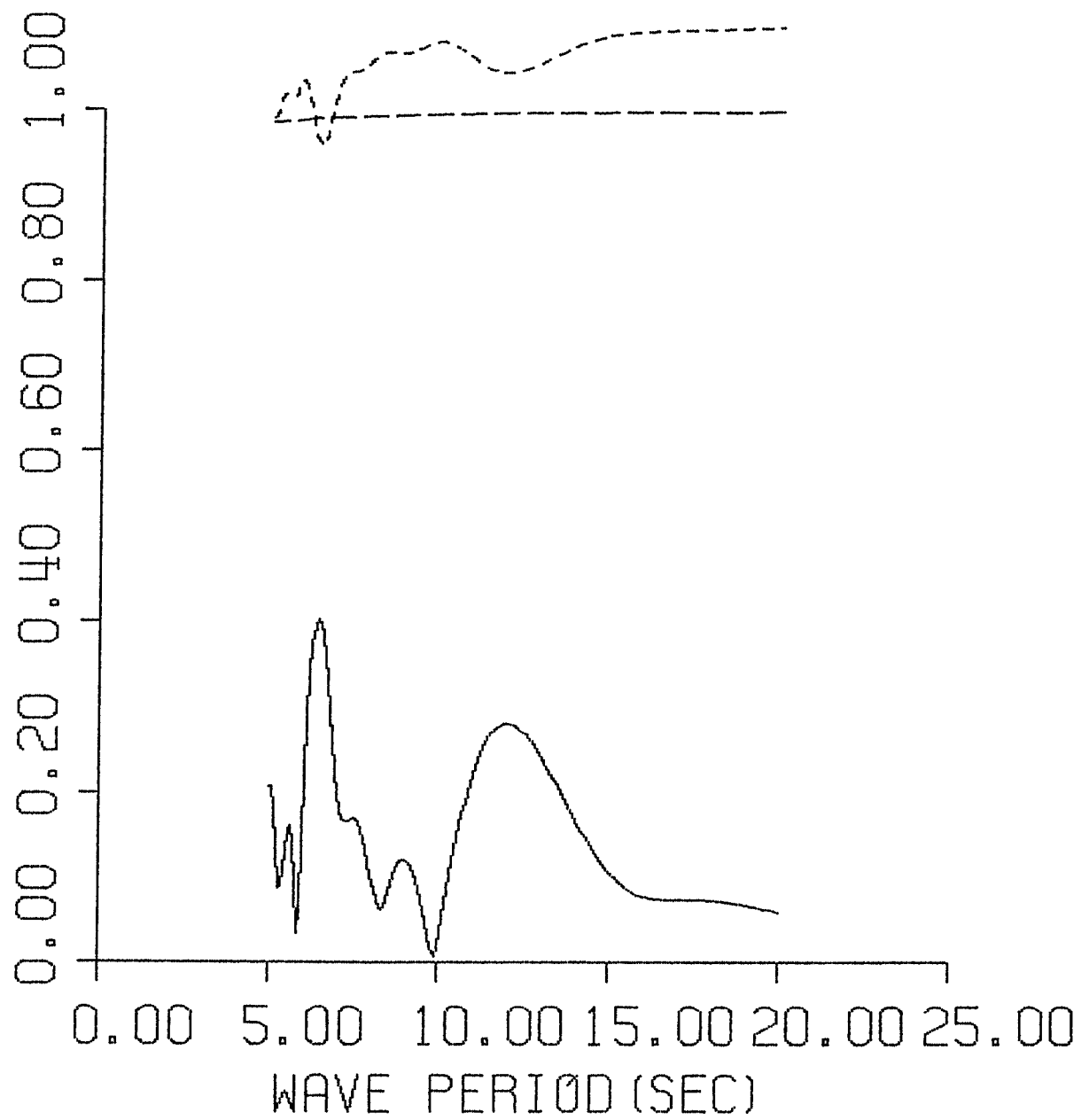
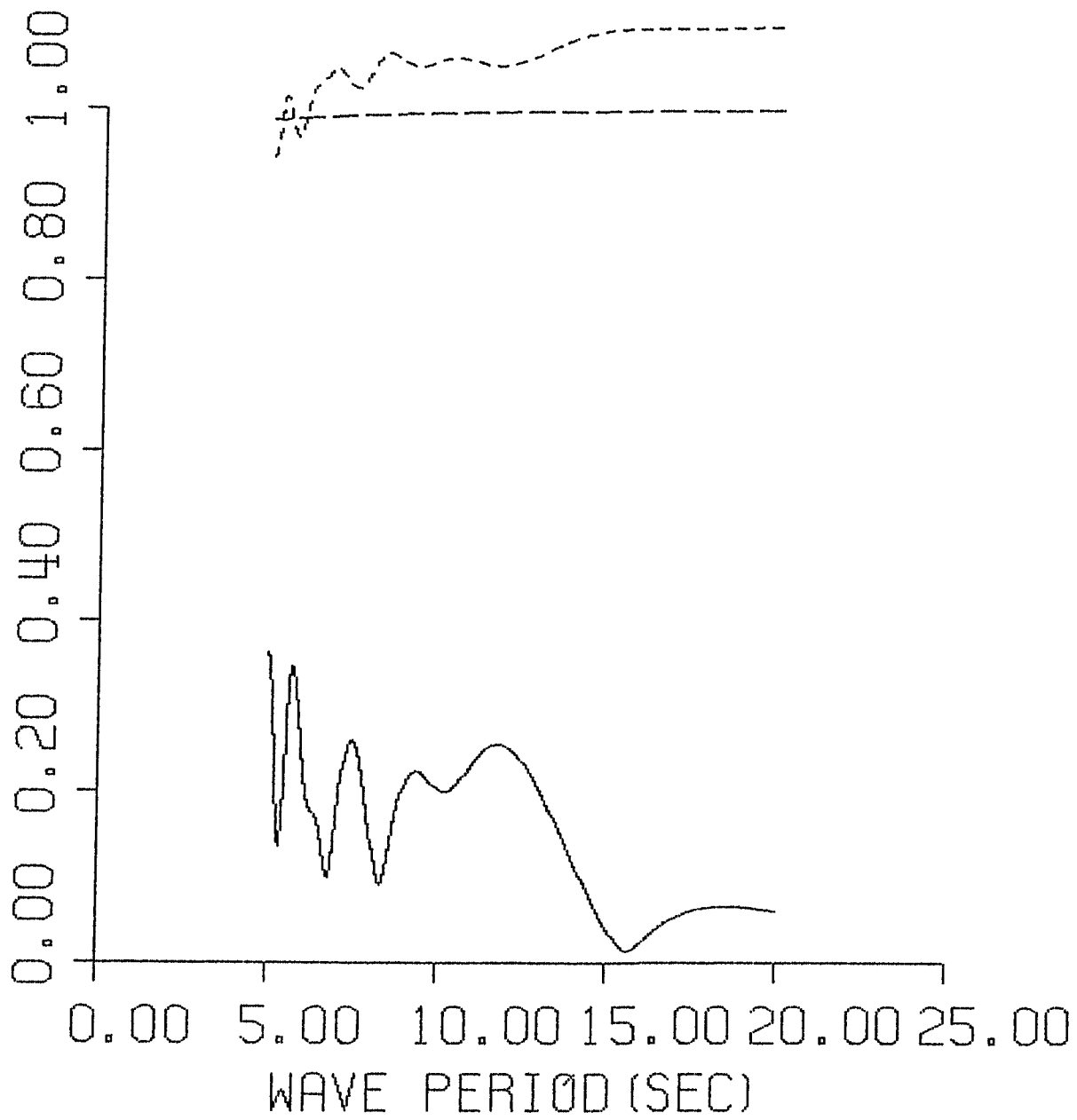


Figure 16. a) 40 - 40 - 40m spacing.



b) 30 - 40 - 50m spacing.

Figure 16: Reflection and transmission for regular and irregular bar spacing on a sloping beach. Four bars, LLW+1.61m.

5 Program Listing

The program corresponding to the theory and numerical algorithm of sections 2 and 3 is given here. The program is written using FORTRAN 77 and will compile under VAX VMS FORTRAN or MICRO-SOFT FORTRAN with no alterations. The program is designed to be run interactively, and prompts the user for all input data values in a self-explanatory way.

The program is organized as a main program which calls a subroutine DEPTH to establish the one-dimensional topography $h(x)$, and subroutine DELDET to establish the perturbation $\delta(x)$. A separate version of DEPTH and DELDET is supplied for each particular topographic form, and the appropriate version thus needs to be linked to the main program during compilation. Additional subroutines called by the main program are WVNUM, which computes the wavenumber k at each grid point, and CTRIDA, which performs the double-sweep solution for the complex-valued tridiagonal system of equations. The main program and WVNUM and CTRIDA are included in the file PROFREF.FOR. Different versions of DEPTH and DELDET are supplied in separate numbered files. Listings of all programs are given below.

The program creates two data files. The file DEPTH.DAT contains the x-coordinate and total depth $h'(x)$ for each grid point. This file may be read by the statements

```
DO I=1,N
  READ(unit,*) X(I),D(I)
END DO
```

where N is the number of grid points as specified in the input to the program.

The second data file REFLEC.DAT contains values of wavenumber k^1 , wave period T , wave angle θ , transmission coefficient $|T|$, reflection coefficient $|R|$ and the energy conservation test value for each computed reflection case. The values of transmission and reflection are based on assuming a white incident wave spectrum, and a true reflected spectrum may

thus be computed by multiplying the incident spectrum at the offshore end of the bar field by the values of $|R|(T, \theta)$. The data file REFLEC.DAT may be read by the statements

```
DO I=1, NP
DO J=1, NDIR
READ(unit, *) K, PERIOD, ANGLE, T, R, TEST
END DO
```

where NP is the number of wave periods and NDIR is the number of wave directions, as specified in program input.

Main program.

```
C*-----
C*   REFLEC1.FOR
C*
C*   PROGRAM COMPUTES THE REFLECTION COEFFICIENT FOR WAVES OVER AN
C*   ARBITRARY BOTTOM WHICH VARIES ONLY IN THE X-DIRECTION.  THE
C*   APPROXIMATION USED IS GIVEN BY KIRBY(1986), JFM, AND ASSUMES
C*   A SLOWLY VARYING TOPOGRAPHY WITH SUPERIMPOSED, FAST SMALL-
C*   AMPLITUDE VARIATIONS.
C*
C*   THE PROGRAM SOLVES THE FULL ELLIPTIC PROBLEM USING CENTERED
C*   FINITE-DIFFERENCES AND A TRIDIAGONAL ELIMINATION SCHEME.  ONE
C*   DIRECTIONAL AND FREQUENCY COMPONENT IS HANDLED AT A TIME.  THE
C*   PROVISION FOR BUILDING UP SPECTRA BY MEANS OF MULTIPLE RUNS IS
C*   INCLUDED.  WAVES ARE ASSUMED TO BE UNBROKEN, NONLINEARITY IS
C*   NEGLECTED, AND BOTTOM DAMPING IS IGNORED.
C*
C*   JAMES KIRBY, JANUARY 1987
C*-----
      PARAMETER(IP=1000)
      COMMON/BLOCK1/H(IP),DEL(IP),K(IP),GAM(IP),P(IP)
      COMMON/BLOCK2/A(IP),B(IP),C(IP),D(IP),V(IP),PHI(IP),ONE
      REAL L,K,M
      DIMENSION ANGLE(20)
      COMPLEX ALF1,ALFN,A,B,C,D,PHI,ONE,V,L1,L2
      OPEN(8,FILE='REFLEC.DAT',STATUS='NEW')
C*-----
C*   ENTRY OF MILDLY SLOPING BOTTOM
C*-----
      CALL DEPTH(L,N,DX)
C*-----
C*   ENTRY OF BOTTOM PERTURBATION INFORMATION
C*-----
      CALL DELDET(L,N,DX)
C*-----
C*   DEFINE NONVARIABLE CONSTANTS
C*-----
      ONE=CMPLX(1.,0.)
      G=9.80621
      PI=3.1415927
      DO 1 I=2,N
      D(I)=CMPLX(0.,0.)
1      CONTINUE
C*-----
C*   SPECIFY WHETHER MULTIPLE RUNS ARE TO BE DONE
C*-----
      WRITE(*,90)
90      FORMAT(' ENTER NUMBER OF PERIODS, TMIN,TMAX')
      READ(*,*) NP,TMIN,TMAX
      DT=(TMAX-TMIN)/(NP-1)
      PERIOD=TMIN
      WRITE(*,91)
91      FORMAT(' ENTER NUMBER OF DIRECTIONAL COMPONENTS')
      READ(*,*) NDIR
```

```

DO 92 IDIR=1,NDIR
WRITE(*,10)IDIR
10  FORMAT(' INPUT ANGLE FOR ', I2,'TH COMPONENT')
    READ(*,*)ANGLE(IDIR)
92  CONTINUE
    DO 300 INP=1,NP
    OMEG=2.*PI/PERIOD
C*-----
C*  SET UP PARAMETERS FOR A GIVEN FREQUENCY RUN
C*-----
    DO 2 I=1,N
    CALL WVNUM(H(I),K(I),OMEG)
    TKH=2.*K(I)*H(I)
    P(I)=OMEG*OMEG*(1.+TKH/SINH(TKH))/(2.*K(I)*K(I))
    GAM(I)=G/(COSH(K(I)*H(I))**.2.)
2   CONTINUE
    DO 3 I=2,N-1
    C(I)=P(I+1)+P(I)-GAM(I)*(DEL(I+1)+DEL(I))
    A(I)=P(I)+P(I-1)-GAM(I)*(DEL(I)+DEL(I-1))
3   CONTINUE
C*-----
C*  SET UP PARAMETERS FOR A GIVEN DIRECTIONAL RUN
C*-----
    DO 290 IDIR=1,NDIR
    THET=PI*ANGLE(IDIR)/180.
    M=K(1)*SIN(THET)
    L1=CSQRT(CMPLX(K(1)*K(1)-M*M,0.))
    L2=CSQRT(CMPLX(K(N)*K(N)-M*M,0.))
    ALF1=L1*DX*CMPLX(0.,1.)/2.
    ALFN=L2*DX*CMPLX(0.,1.)/2.
    B(1)=-ONE+ALF1
    C(1)=ONE+ALF1
    D(1)=2.*ALF1*(CEXP(2.*ALF1)+ONE)
    A(N)=-ONE-ALFN
    B(N)=ONE-ALFN
    DO 4 I=2,N-1
    B(I)=- (A(I)+C(I))+CMPLX(2.*DX*DX*((K(I)*K(I)-M*M)*P(I)+M*M*
1GAM(I)*DEL(I)),0.)
4   CONTINUE
C*-----
C*  OBTAIN WAVE FIELD
C*-----
    CALL CTRIDA(1,N)
    DO 5 I=1,N
    PHI(I)=V(I)
5   CONTINUE
C*-----
C*  REFLECTION AND TRANSMISSION COEFFICIENTS
C*-----
    T1=CABS(PHI(N))
    T2=CABS(PHI(N-1))
    R1=CABS(PHI(1)-ONE)
    R2=CABS(PHI(2)-CEXP(2.*ALF1))
    WRITE(*,*)R1,R2,R1-R2

```

```
WRITE(*,*)T1,T2,T1-T2
T=(T1+T2)/2.
R=(R1+R2)/2.
TEST=((K(N)*P(N))/(K(1)*P(1)))*T*T+R*R
WRITE(*,*)T,R,TEST
```

```
C*-----
```

```
C*   STORE RESULTS AND MOVE ON TO NEXT COMPONENT
```

```
C*-----
```

```
WRITE(8,*) K(1),PERIOD,ANGLE(IDIR),T,R,TEST
290 CONTINUE
PERIOD=PERIOD+DT
300 CONTINUE
CLOSE(8)
STOP
END
```

Subroutine WVNUM

```
C*-----  
C*  
C*      SUBROUTINE WVNUM(D,K,S)  
C*  
C*      CALCULATE WAVENUMBER K ACCORDING TO THE FORM  
C*  
C*          S*S-G*K*TANH(K*D)=0.  
C*  
C*      WHERE  
C*  
C*          D   = LOCAL WATER DEPTH  
C*          S   = ABSOLUTE FREQUENCY  
C*          G   = GRAVITATIONAL ACCELERATION CONSTANT  
C*  
C*      SOLUTION BY NEWTON-RAPHSON ITERATION USING ECKART'S  
C*      APPROXIMATION AS A SEED VALUE.  
C*-----  
      REAL K,KN  
      G=9.80621  
      PI=3.1415927  
      K=S*S/(G*SQRT(TANH(S*S*D/G)))  
      DO 1 II=1,20  
      F=S*S-G*K*TANH(K*D)  
      FP=-G*TANH(K*D)-G*K*D/(COSH(K*D)**2.)  
      KN=K-F/FP  
      IF((ABS(KN-K)/KN).LT.EPS)GO TO 2  
      K=KN  
1     CONTINUE  
      T=2.*PI/(SQRT(G*K*TANH(K*D)))  
      RETURN  
2     K=KN  
      RETURN  
      END
```

Subroutine CTRIDA

```
C*-----
C*
C*      SUBROUTINE CTRIDA(IF,L)
C*
C*      TRIDIAGONAL MATRIX SOLUTION BY DOUBLE SWEEP ALGORITHM. PRESENT
C*      SUBROUTINE ADOPTED FROM THE SUBROUTINE DESCRIBED IN:
C*
C*          CARNAHAN, LUTHER AND WILKES, APPLIED NUMERICAL
C*          METHODS, WILEY, 1969
C*
C*      MODIFIED TO HANDLE COMPLEX ARRAY COEFFICIENTS AND SOLUTION
C*      VALUES. INPUT AND OUTPUT ARE
C*
C*          A,B,C = COEFFICIENTS OF ROW IN TRIDIAGONAL MATRIX
C*          D     = RIGHT HAND SIDE VECTOR OF MATRIX EQUATION
C*          V     = SOLUTION VECTOR
C*          IF,L  = BEGINNING AND END INDICES OF POSITIONS IN THE
C*                DIMENSIONED RANGE OF THE COLUMN VECTOR TO BE
C*                CONSIDERED.
C*-----
C*      PARAMETER(IP=1000)
C*      COMMON/BLOCK2/A(IP),B(IP),C(IP),D(IP),V(IP),PHI(IP),ONE
C*      COMPLEX A,B,C,D,PHI,ONE,V
C*      COMPLEX BETA(IP),GAMMA(IP)
C*-----
C*      COMPUTE INTERMEDIATE VECTORS BETA AND GAMMA
C*-----
C*      BETA(IF)=B(IF)
C*      GAMMA(IF)=D(IF)/BETA(IF)
C*      IFP1=IF+1
C*      DO 1 I=IFP1,L
C*      BETA(I)=B(I)-A(I)*C(I-1)/BETA(I-1)
C*      GAMMA(I)=(D(I)-A(I)*GAMMA(I-1))/BETA(I)
C*      1 CONTINUE
C*-----
C*      COMPUTE SOLUTION VECTOR V
C*-----
C*      V(L)=GAMMA(L)
C*      LAST=L-IF
C*      DO 2 K=1, LAST
C*      I=L-K
C*      V(I)=GAMMA(I)-C(I)*V(I+1)/BETA(I)
C*      2 CONTINUE
C*      RETURN
C*      END
```

Subroutine DEPTH

a) Version DEPTH1.FOR; flat bottom

```
C*-----
C*  DEPTH1.FOR
C*
C*  SUBROUTINE DEPTH(L,N,DX)
C*
C*  DEPTH MODULE 1: SIMPLE UNIFORM DEPTH HO
C*-----
      PARAMETER (IP=1000)
      COMMON/BLOCK1/H(IP),DEL(IP),K(IP),GAM(IP),P(IP)
      REAL L,K,M
      WRITE(*,1)
1  FORMAT(' ENTER UNIFORM DEPTH HO')
      READ(*,*) HO
      WRITE(*,3)
3  FORMAT(' ENTER DOMAIN LENGTH L, NUMBER OF POINTS N')
      READ(*,*)L,N
      DX=L/FLOAT(N-1)
      DO 2 I=1,N
      H(I)=HO
2  CONTINUE
      RETURN
      END
```

b) Version DEPTH2.FOR; sloping bottom

```
C*-----
C*  DEPTH2.FOR
C*
C*  SUBROUTINE DEPTH(L,N,DX)
C*
C*  DEPTH MODULE 2: SIMPLE PLANE SLOPE
C*-----
      PARAMETER (IP=1000)
      COMMON/BLOCK1/H(IP),K(IP),GAM(IP),P(IP)
      REAL L,K,M
      WRITE(*,1)
1  FORMAT(' ENTER DOMAIN LENGTH L, DEEP DEPTH H1,SHALLOW DEPTH H2')
      READ(*,*)L,H1,H2
      SLOPE=(H1-H2)/L
      WRITE(*,2)
2  FORMAT(' ENTER NUMBER OF POINTS N')
      READ(*,*) N
      DX=L/FLOAT(N-1)
      DO 3 I=1,N
      H(I)=H1-SLOPE*FLOAT(I-1)*DX
3  CONTINUE
      H(1)=H(2)
      H(N)=H(N-1)
      RETURN
      END
```

Subroutine DELDET
a) Version DELDET1.FOR; semicircular bars

```
C*-----  
C*  
C*   DELDET1.FOR  
C*  
C*   SUBROUTINE DELDET(L,N,DX)  
C*  
C*   DEL MODULE 1: SEMICIRCULAR BARS  
C*-----  
      PARAMETER(IP=1000)  
      COMMON/BLOCK1/H(IP),DEL(IP),K(IP),GAM(IP),P(IP)  
      REAL L,K,M  
      DIMENSION X(IP)  
      DO 1 I=1,N  
        DEL(I)=0.  
        X(I)=FLOAT(I-1)*DX  
1      CONTINUE  
        WRITE(*,2)  
2      FORMAT(' ENTER NUMBER OF BARS')  
        READ(*,*)NBARS  
        IF(NBARS.EQ.0)GO TO 7  
        WRITE(*,3)  
3      FORMAT(' INPUT XO,RO FOR EACH BAR [ONE PAIR PER LINE]')  
        DO 5 J=1,NBARS  
          READ(*,*)XO,RO  
          DO 4 I=1,N  
            IF(ABS(X(I)-XO).LE.RO)THEN  
              DEL(I)=DEL(I)+SQRT(RO*RO-(X(I)-XO)**2)  
            ENDIF  
4          CONTINUE  
5          CONTINUE  
C*-----  
C*   STORE TOTAL DEPTH  
C*-----  
7      OPEN(9,FILE='DEPTH.DAT',STATUS='NEW')  
        DO 6 I=1,N  
          D=H(I)-DEL(I)  
          WRITE(9,*) X(I),D  
6      CONTINUE  
        CLOSE(9)  
        RETURN  
        END
```

b) Version DELDET2.FOR; sinusoidal bars

```
C*-----
C*
C*   DELDET2.FOR
C*
C*   SUBROUTINE DELDET(L,N,DX)
C*
C*   DEL MODULE 2: SINUSOIDAL BARS
C*-----
      PARAMETER(IP=1000)
      COMMON/BLOCK1/H(IP),DEL(IP),K(IP),GAM(IP),P(IP)
      REAL L,K,M
      DIMENSION X(IP)
      PI=3.1415927
      DO 1 I=1,N
      DEL(I)=0.
      X(I)=FLOAT(I-1)*DX
1      CONTINUE
      WRITE(*,2)
2      FORMAT(' ENTER NUMBER OF BARS')
      READ(*,*)NBARS
      IF(NBARS.EQ.0)GO TO 7
      WRITE(*,3)
3      FORMAT(' INPUT XO, BAR LENGTH, AND BAR AMPLITUDE')
      READ(*,*)XO,BARL,BARD
      DO 4 I=1,N
      IF(((X(I)-XO).GT.0.).AND.((X(I)-XO).LE.(NBARS*BARL)))THEN
      DEL(I)=BARD*SIN(2.*PI*(X(I)-XO)/BARL)
      ENDIF
4      CONTINUE
C*-----
C*   STORE TOTAL DEPTH
C*-----
7      OPEN(9,FILE='DEPTH.DAT',STATUS='NEW')
      DO 6 I=1,N
      D=H(I)-DEL(I)
      WRITE(9,*) X(I),D
6      CONTINUE
      RETURN
      END
```

6 References

1. Berkhoff, J.C.W., 1972, "Computation of combined refraction - diffraction", *Proc. 13th Int. Conf. Coastal Eng.*, Vancouver, 471-490.
2. Carnahan, B., Luther, H.A. and Wilkes, J.O., 1969, *Applied Numerical Methods*, John Wiley
3. Dalrymple, R.A. and Kirby, J.T., "Water waves over ripples" *Journal of Waterway, Port, Coastal and Ocean Engineering* 112, 309-319.
4. Davies, A.G. and Heathershaw, A.D., 1984, "Surface - wave propagation over sinusoidally varying topography" *Journal of Fluid Mechanics* 144, 419-443.
5. DeVries, J., 1987, "Bragg reflection - notes on field study preparation", Naval Civil Engineering Laboratory, unpublished planning document.
6. Kirby, J.T., 1986, "A general wave equation for waves over rippled beds" *Journal of Fluid Mechanics* 162, 171-186.
7. Mei, C.C., 1985, "Resonant reflection of surface water waves by periodic sand bars" *Journal of Fluid Mechanics* 152, 315-335.
8. Miles, J.W., 1981 "Oblique surface-wave diffraction by a cylindrical obstacle", *Dynamics of Atmospheres and Oceans* 6, 121-123.